Supramolecular Polymers Generated from Heterocomplementary Monomers Linked through Multiple Hydrogen-Bonding Arrays—Formation, Characterization, and Properties

Volker Berl,[a, b] Marc Schmutz,[c] Michael J. Krische,[a, d] Richard G. Khoury,[a] and Jean-Marie Lehn*[a]

Dedicated to the memory of Darshan Ranganathan

Abstract: Supramolecular polymers are described that are derived from the association of two homoditopic heterocomplementary monomers through sextuple hydrogen-bonding arrays. They form fibers and a variety of different materials depending on the conditions. The strong affinity of the DAD – DAD (D = donor, A = acceptor) hydrogen-bonding sites for double-faced cyanuric acid type wedges drives the supramolecular polymeric assembly in apolar and chlorinated organic solvents. The marked influence of stoichiometry, as well as end-capping and cross-linking agents upon fiber formation is revealed in solution and by electron microscopy (EM). The results further contribute to the development of a supramolecular polymer chemistry that comprizes reversible polymers formed through recognition-controlled noncovalent connections between the molecular components. Such materials are, by nature, dynamic and present adaptive character in view of their ability to respond to external stimuli.

Keywords: dynamic materials · hydrogen bonds · polymers · self-assembly · supramolecular chemistry

Introduction

Unlike covalent polymers, supramolecular polymers are materials that result from the association of the monomeric components through noncovalent interactions rather than by the formation of covalent bonds through polymerization reactions. As the properties of a material depend both on the nature of its constituents and on the interactions between them, molecular recognition processes occurring at the molecular level induce changes in the physical properties of a substance at the macroscopic level. Such changes in the macroscopic properties may involve phase organization, viscosity, optical properties, etc., thus demonstrating the potential of supramolecular materials chemistry for creating noncovalent materials with novel properties. The emerging area of supramolecular polymer chemistry has been put into perspective,[1–3] and reviewed.[4–9]

The field of supramolecular materials covers all materials whose molecular components are connected through *reversible* noncovalent interactions so that they spontaneously and continuously undergo dynamic self-assembly and disassembly processes. This feature confers dynamic character on these materials, so that supramolecular materials may be considered to be, in effect, *dynamic materials*.[3, 9b] In a broader perspective, dynamic materials can be of a molecular or supramolecular nature depending on whether the reversible connections are covalent or noncovalent.

Another feature of dynamic materials arises from their ability to exchange their constituents. Dynamic materials can therefore be viewed as combinatorial systems, whose constituents have combinatorial diversity and may, in principle, be expressed differently in response to external or environmental factors, a feature that confers adaptive character on the material.[3, 9b, 10]

[a] Prof. Dr. J.-M. Lehn, Dr. V. Berl, Dr. M. J. Krische, Dr. R. G. Khoury
Laboratoire de Chimie Supramoléculaire
ESA 7006 of the CNRS, ISIS, Université Louis Pasteur
4 rue Blaise Pascal, 67000 Strasbourg (France)
Fax: (+33) 3-90-24-11-17
E-mail: lehn@chimie.u-strasbg.fr

[b] Dr. V. Berl
Affiliated institution: Forschungszentrum Karlsruhe GmbH
Institut für Nanotechnologie, Postfach 3640, 76021 Karlsruhe (Germany)

[c] Dr. M. Schmutz
Institut de Génétique et de Biologie Moléculaire et Cellulaire
CNRS/INSERM/ULP
B. P. 163, C. U. de Strasbourg, 67404 Illkirch (France)
Present address: Institut Charles Sadron, CNRS-ULP
6 rue Boussingault, 67083 Strasbourg (France)

[d] Dr. M. J. Krische
Present address: University of Texas at Austin
Department of Chemistry and Biochemistry, Austin, TX 78712 (USA)

  0947-6539/02/0805-1227 $ 17.50+.50/0

Supramolecular polymers can be regarded as a subclass of such adaptive, dynamic combinatorial materials, as they are capable of growing and shortening, of exchanging their components, and of rearranging their structure. Unlike covalent polymers, which incorporate the defects of their formation permanently, supramolecular polymers have dynamic features such as self-repairing and self-healing.[2] Specific additives, interacting with the molecular recognition motifs on the basis of their polyassociation, may allow the control of features such as growth and cross-linking within the supramolecular polymeric framework.

As part of a research program on H-bond-mediated self-assembly,[1, 11] our investigations concerned in particular "bottom-up" approaches to liquid crystalline materials and liquid crystalline polymers that possess noncovalent main chains.

The hierarchical generation of mesophases through the H-bond-mediated association of complementary components has been realized first with complementary ADA and DAD arrays of triple hydrogen-bonding donor (D) and acceptor (A) sites through heterocyclic derivatives of diaminopyridine (P) and uracil (U).[12] Molecular-recognition-induced self-assembly leads to a supramolecular liquid crystalline polymer of triple helical superstructure, generated from the heterocomplementary homoditopic molecular monomers, via triple hydrogen-bonding arrays,[13, 14] to rigid-rod supramolecular polymer systems.[15] Supramolecular discotic liquid crystals have also been obtained through the self-assembly of sector components into trimeric disk-like structures, which subsequently self-organize into a thermotropic discotic columnar mesophase, by following a hierarchical self-organization process.[16] Moreover, mesophases could be formed from a combination of monotopic and ditopic complementary components.[17]

Supramolecular arrays that have pendent, flexible side chains were prepared by the hydrogen-bonding recognition between homo-[18] and heterocomplementary[19] double-faced Janus type heterocyclic units, forming ordered molecular solids through the assembly of polyassociated supramolecular strands. Components containing such Janus type molecular-recognition groups (cyanuric or barbituric acid and triaminopyridine or triaminotriazine derivatives) have been used for the self-assembly of a variety of supramolecular architectures,[20] as well as for inducing selective interactions between vesicles[21a] and at interfaces with molecular layers.[21b] If two of these recognition groups are grafted onto a tartaric acid spacer, ditopic molecular monomers are generated that form very high molecular weight aggregates, which can be characterized by various physical methods.[22]

A number of main chain supramolecular polymeric systems that assemble through single to quadruple hydrogen-bonding arrays,[23–36] and metal ion–ligand coordination[37–39] have been described. In particular, the use of self-complementary DDAA quadruply hydrogen-bonding arrays allowed the generation of supramolecular polymers of significant lengths in dilute isotropic solutions and that display features of interest for materials, such as a highly concentration- and temperature-dependent viscosity, which are attributed to changes in polymer length, as well as end-capping and cross-linking processes.[23, 24]

Design strategy: We searched for purely organic systems, in which the molecular-recognition-driven polyassociation of monomers would be ensured by a well-defined hydrogen-bonded pattern of complementary units. Previous examples have strongly favored this type of supramolecular interaction as it combines simplicity with directionality (see references above).

The high association constants expected from the formation of six hydrogen bonds suggested the use of a Janus type cyanuric wedge (ADA-ADA-array) (**B**) and a corresponding diaminopyridine-substituted isophthalamide receptor (DAD–DAD array) (**A**) as ditopic complementary monomers (Figure 1).

Two types of ditopic monomeric species that employ these units **A** and **B** can be devised in order to generate a main chain supramolecular polymer: either self-associating heteroditopic

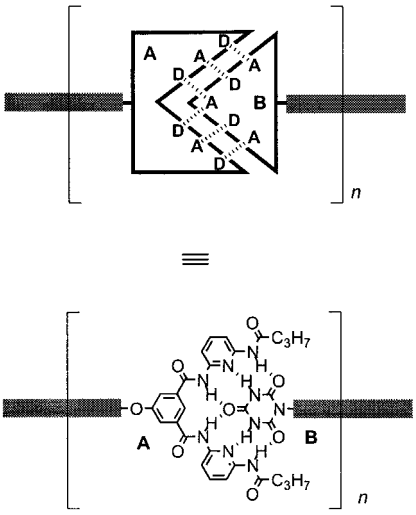

Figure 1. Choice of the complementary hydrogen-bonded molecular recognition units.

Abstract in French: *Des polymères supramoléculaires ont été obtenus par polyassociation de deux monomères homoditopiques hétérocomplémentaires liés par un réseau de six liaisons hydrogène. Ils forment des fibres et une variété de matériaux en fonction des conditions. La grande affinité des sites de reconnaissance par liaison hydrogène DAD–DAD pour le groupe cyanurique à double-face complémentaire commande l'autoassemblage du polymère supramoléculaire. L'effet prononcé de la stoechiométrie ainsi que celui d'agents de terminaison et de réticulation sur la formation des fibres est mis en évidence en solution et par microscopie électronique. Les résultats obtenus contribuent au développement d'une chimie des polymères supramoléculaires, concernant les polymères réversibles formés par la connexion noncovalente de composants moléculaires sur la base de processus de reconnaissance moléculaire. De tels matériaux sont par nature dynamiques, et présentent un caractère adaptatif du fait de leur capacité à réagir à des stimuli externes.*

  0947-6539/02/0805-1228 $ 17.50+.50/0 *Chem. Eur. J.* **2002**, *8*, No. 5

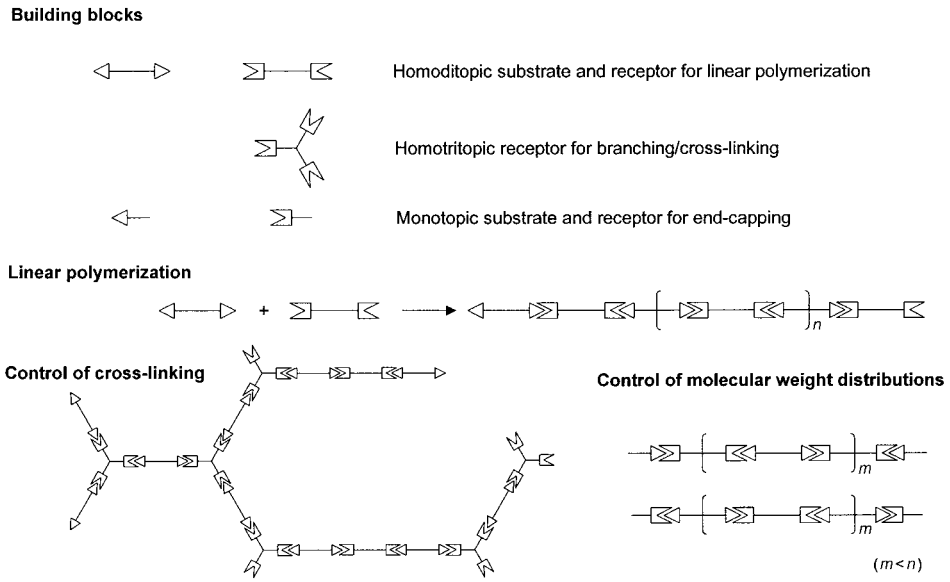

Figure 2. Aspects of the chemistry of supramolecular polymers; schematic representation of the complementary monomeric building blocks.

monomers (**AB**) or two-component mixtures of heterocomplementary homoditopic monomers (**AA** plus **BB**). Polyassociation of **AB**-type monomers yields supramolecular homopolymers; initiation and growth occur immediately after generation of the recognition groups. On the other hand, regularly alternating supramolecular heteropolymers are formed upon mixing stoichiometric ratios of **AA** and **BB**.

The latter two-component system was chosen for several reasons: a) the symmetrically substituted monomers would be easier to prepare and to characterize; b) the control of the extent of polymerization through slight stoichiometric imbalances between **AA** and **BB** presents an additional level of control compared with the uncontrolled **AB**-type polymerization, which requires additional chain-stopper molecules; and c) the facile design of two-dimensional and three-dimensional cross-linking agents can be envisaged.

Figure 2 schematically presents different features that such polymeric assemblies may exhibit (see also ref. [9b]): linear polymerization, insured by the polyassociation of the homoditopic receptor **AA** and the substrate **BB**; branching through a dendritic, homotritopic receptor; controlling the extent of cross-linking in the linear polymer chains; and various means of achieving molecular weight control, such as employing **AA** and **BB** in nonstoichiometric ratios or using substances bearing a single recognition group as chain stoppers.

The design of the molecular backbone of the monomers is also important, as it will have a strong influence on the polymer properties. Thermal stability and compatibility with the hydrogen-bonding motifs are two requirements. Ease of synthesis and versatility of functionalization are also desirable. A simple 1,3-dioxopropane spacer was used to connect the receptor recognition groups in component **1**, **AA** (Scheme 1). The construction of the tritopic branching agent **2** was achieved by using a mesitylenic spacer to link three receptor recognition groups through ether functions. A chiral tartaric acid spacer, in which the hydroxyl functions are alkylated by an aliphatic chain, was employed to connect two Janus-wedge subunits in component **3**, **BB**. The terminal butyryl amides of the receptors were introduced to ensure solubility in chlorinated solvents. The polar cyanuric recognition groups of bis-wedge **3** are solubilized by long alkyl chains on the tartaric linker.[13] The monotopic species **4**, **4b**, and **13** may serve as chain termination components. Formation of six hydrogen bonds between the complementary recognition groups **A** and **B** of the ditopic monomeric components **1**, **AA** and **3**, **BB**, is expected to generate the linear supramolecular polymer represented in Scheme 2.

Results and Discussion

Synthesis of the molecular components: A modular and convergent route for the synthesis of the cyanuric acid based bis-receptor **1** and trisreceptor **2** was developed to facilitate access to preparative quantities of these materials (Scheme 3).

O-Alkylation of dimethyl 5-hydroxyisophthalate **5** was accomplished with 1,3-dibromopropane or 1,3,5-tris(bromomethyl)benzene (**7**) to yield tetraester **9** or hexaester **11**, respectively. 1,3,5-Tris(bromomethyl)benzene was prepared from mesitylene by a radical allylic bromination step. Esters **9** and **11** were subsequently hydrolyzed to their corresponding carboxylic acids, **10** and **12**, and converted to the acid chlorides, **10b** and **12b**. Treatment of the acid chlorides with previously prepared *N*-(6-aminopyridin-2-yl)butyramide (**8**) afforded receptors **1** and **2** in good yields. Monoamide **8** was obtained by statistical acylation of 2,6-diaminopyridine **6** with butyryl chloride.

Synthesis of the L-tartaric bis-cyanurate **3** (also termed bis-wedge **3**) was achieved by following procedures developed in other work.[13, 40] The preparation of **4**, **4b** and **13** is indicated in the Experimental Section.

Solution studies on the polymeric assemblies:

Determination of the association constants: In order to be able to evaluate the extent of polymerization in solution upon mixing bis-wedge **3** with bis-receptor **1** or with trisreceptor **2**, knowledge of the association constants of the systems is required. For a supramolecular polymeric assembly, determination of the binding constants is a priori not possible due to the underlying complex system of equilibria, which involves a great variety of equilibrating species. However, it can be assumed that the two cyanuric binding heads of the ditopic wedge **3** exhibit an affinity for the polytopic receptors **1** and **2** comparable to that of the corresponding monotopic cyanurate wedge **4**. Thus, a series of titration studies was conducted in chloroform, by progressive addition of **4** to a dilute solution of

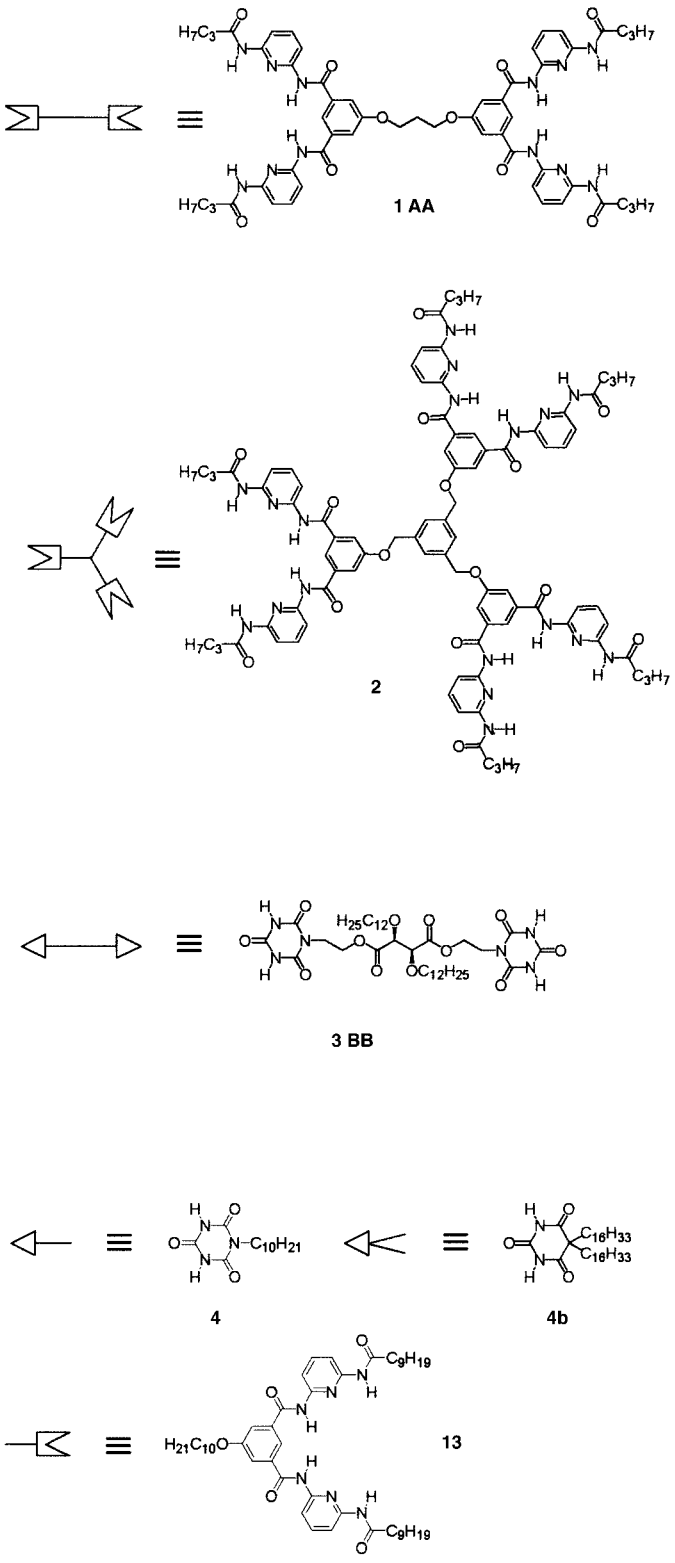

Scheme 1. Molecular components.

1, **2**, and **13**. The chemical shifts of selected proton signals were monitored, and the data sets obtained were used as input for the calculations of the constants, with the computer program *Chem-Equili*.[41]

The following chart summarizes the equilibrium models applied and the results of the *Chem-Equili* calculations. The association constants obtained are in good agreement with the order of magnitude reported for similar systems.[42, 43]

Monoreceptor:	
$[\mathbf{13}]+[\mathbf{4}] \rightleftharpoons [\mathbf{13}{:}\mathbf{4}]$	$\log K_a = 4.8\ (\pm 0.04)$
Bis-receptor:	
$[\mathbf{1}]+[\mathbf{4}] \rightleftharpoons [\mathbf{1}{:}\mathbf{4}]$ (at 50 °C)	$\log K_a = 4.2\ (\pm 0.4)$
$[\mathbf{1}]+2[\mathbf{4}] \rightleftharpoons [\mathbf{1}{:}\mathbf{4}_2]$	$\log K_{a2} = 7.8\ (\pm 0.3)$
$([\mathbf{1}{:}\mathbf{4}]+[\mathbf{4}] \rightleftharpoons [\mathbf{1}{:}\mathbf{4}_2]$	$\log K_{a2}' = 3.6)$
Trisreceptor:	
$[\mathbf{2}]+[\mathbf{4}] \rightleftharpoons [\mathbf{2}{:}\mathbf{4}]$	$\log K_{a1} = 4.6\ (\pm 0.9)$
$[\mathbf{2}]+2[\mathbf{4}] \rightleftharpoons [\mathbf{2}{:}\mathbf{4}_2]$	$\log K_{a2} = 8.8\ (\pm 0.6)$
$[\mathbf{2}]+3[\mathbf{4}] \rightleftharpoons [\mathbf{2}{:}\mathbf{4}_3]$	$\log K_{a3} = 13.4\ (\pm 1.0)$
$([\mathbf{2}{:}\mathbf{4}]+[\mathbf{4}] \rightleftharpoons [\mathbf{2}{:}\mathbf{4}_2]$	$\log K_{a2}' = 4.2\ )$
$([\mathbf{2}{:}\mathbf{4}_2]+[\mathbf{4}] \rightleftharpoons [\mathbf{2}{:}\mathbf{4}_3]$	$\log K_{a3}' = 4.6)$

Analysis of the species distributions in the form of a Scatchard plot of both the three-component $\mathbf{1}{:}\mathbf{4}_2$ and the four-component $\mathbf{2}{:}\mathbf{4}_3$ systems reveals that the binding of the cyanurate to both receptors **1** and **2** presents positive cooperativity.[45] The maximum of the Scatchard curve at $r_{max} = 1.07$ allows the determination of the Hill coefficient:

$$n_H = t/(t - r_{max}) = 1.55 \text{ (for } t = 3)$$

Nuclear magnetic resonance studies—Variable-temperature experiments. Qualitative evidence for aggregate formation: Upon mixing stoichiometric amounts of bis-receptor **1** and bis-wedge **3** in a nonpolar solvent, at 5 mM concentration with respect to each molecular component, the formation of a supramolecular linear polymer $[\mathbf{1}{:}\mathbf{3}]_n$ was anticipated. When a solution of such a mixture in [D_2]tetrachloroethane is heated from −20 °C to 90 °C, the ^{1}H NMR spectra show a significant sharpening of the peaks, due to the partial rupture of the hydrogen bonds that hold the polymeric assemblies together. The rupture of the hydrogen bonds occurs visibly above 50 °C, as suggested by the shifting of the amide proton signals ($\delta =$ 10.0 and 9.2) of the receptor toward higher fields. At low temperature, the H-bond mediated association is much stronger and results in a more highly associated polymeric material, and further aggregation into fibers may set in; this leads to a considerable broadening of the signals (Figure 3a). This effect is even more pronounced if a similar experiment is conducted on the mixture of **2** and **3** in a 1:1.5 molar ratio (5 mM and 7.5 mM, respectively). This can be due to the formation of a polymeric and presumably highly entangled network $[\mathbf{2}{:}\mathbf{3}_{1.5}]_n$ (Figure 3b).

Further support for aggregate formation by the H-bond mediated supramolecular polymerization of molecular components was provided by a series of solution studies that elucidated the behavior of polymers $[\mathbf{1}{:}\mathbf{3}]_n$ and $[\mathbf{2}{:}\mathbf{3}_{1.5}]_n$ upon addition of a branching and an end-capping agent, respectively.

End-capping of the $[\mathbf{2}{:}\mathbf{3}_{1.5}]_n$ *network*: If cyanurate **4** is added portion-wise to a polymeric network of $[\mathbf{2}{:}\mathbf{3}_{1.5}]_n$ (5 mM in [D_2]tetrachloroethane), this monotopic wedge competes with the ditopic cyanurate **3** for occupation of the receptor binding sites. The result is a decrease in the degree of entanglement

  0947-6539/02/0805-1230 $ 17.50+.50/0 *Chem. Eur. J.* **2002**, *8*, No. 5

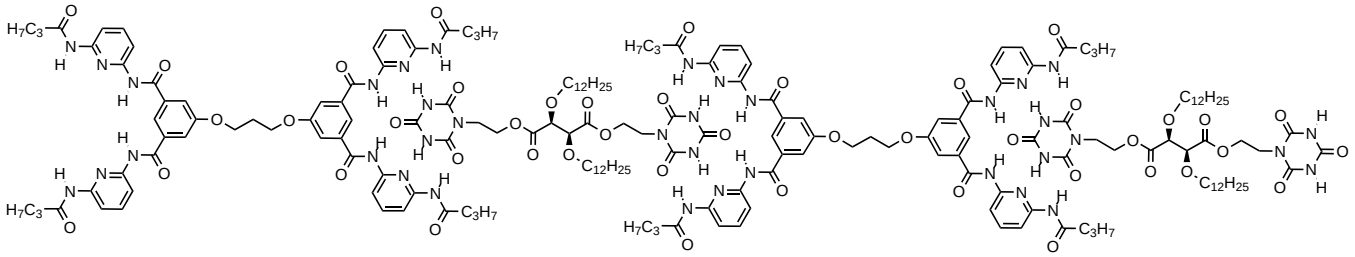

Scheme 2. Linear supramolecular polymer formed by H-bond-mediated molecular recognition between heterocomplementary binding sites of the homoditopic bis-receptor **1**, **AA**, and of the homoditopic bis-wedge substrate **3**, **BB**.

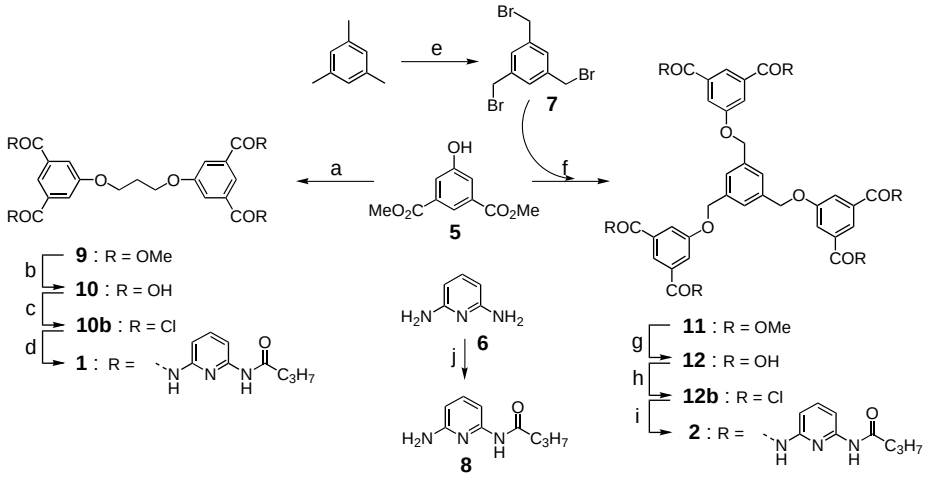

Scheme 3. Synthesis of the homoditopic receptor **1** and of the homotritopic receptor **2**. a) 1,3-Dibromopropane, DMF, K_2CO_3, 60 °C, 80 %; b) NaOH, EtOH/H_2O, reflux, 95 %; c) $SOCl_2$, reflux; d) **8**, Et_3N, THF, 0 °C, 99 %; e) *N*-bromosuccinimide, azobis-(isobutyro)nitrile, CCl_4, $h\nu$, 11 %; f) **7**, DMF, K_2CO_3, 60 °C, 59 %; g) LiOH, H_2O/THF, reflux, 89 %; h) $SOCl_2$, DMF cat., reflux; i) **8**, Et_3N, THF, 0 °C, 87 %; j) butyryl chloride, Et_3N, THF, 0 °C, 60 %.

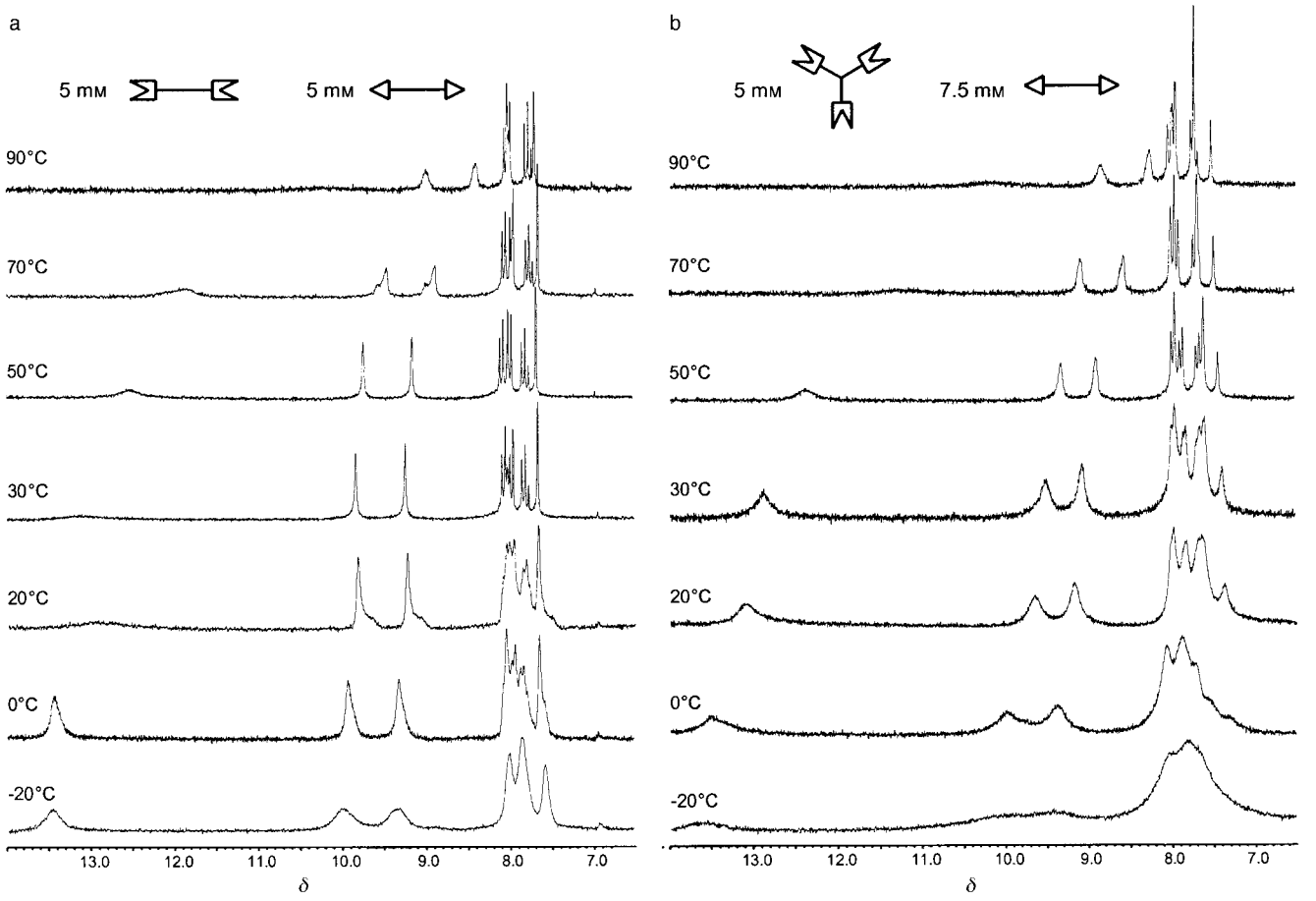

Figure 3. Variable-temperature experiments (5 mM) in [D_2]tetrachloroethane on a) the linear supramolecular polymer $[\mathbf{1}:\mathbf{3}]_n$ and b) the entangled supramolecular network $[\mathbf{2}:\mathbf{3}_{1.5}]_n$ (see Scheme 1).

toward the formation of smaller species, a trend that is supported by the significant sharpening of the initially very ill defined spectrum of $[\mathbf{2}:\mathbf{3}_{1.5}]_n$ with increasing amounts of added **4** (Figure 4a). The addition of an end-capping agent should be equivalent, in a first approximation, to a change in the stoichiometry in favor of **3** in the $[\mathbf{2}:\mathbf{3}_{1.5}]_n$ polymer. This is indeed observed in a ^{1}H NMR experiment involving the portion-wise addition of **3** (at 10 mM) to a mixture of $[\mathbf{2}:\mathbf{3}_{1.5}]_n$ (at 5 mM) in tetrachloroethane. The result is a noticeable sharpening of the signals, similar to that observed for the end-capping experiment (results not shown).

Branching of the linear polymer $[\mathbf{1}:\mathbf{3}]_n$: The inverse trend, the further broadening of the spectra of a stoichiometric mixture of **1** and **3** (2 mM in tetrachloroethane), occurs if the tritopic branching receptor **2** is added. This broadening can be interpreted as the result of a higher degree of cross-linking in the mixture (Figure 4b).

NMR proton relaxation studies in chloroform and NOE experiments: NMR proton-relaxation-time studies supported the formation of higher-molecular-weight aggregates when bis-receptor **1** was mixed with stoichiometric amounts of **3**. T_1 measurements were conducted on solutions of the discrete complex $\mathbf{1}:\mathbf{4}_2$ in [D]chloroform (10 mM) and of the supramolecular polymer $[\mathbf{1}:\mathbf{3}]_n$, at NMR spectrometer frequencies of 200 MHz and 500 MHz. The comparison of the values of T_1 obtained at a given temperature confirmed the formation of higher-molecular-weight aggregates in solution (see Experimental Section).

Viscosity properties: The observation that the supramolecular polymer $[\mathbf{1}:\mathbf{3}]_n$ forms highly viscous solutions in toluene under quite dilute conditions (down to 1 mM, with respect to each molecular component) prompted us to undertake viscosimetric measurements[46] in order to get a deeper insight into the physico-chemical and materials properties of supramolecular polymer $[\mathbf{1}:\mathbf{3}]_n$. At present, only preliminary rheological studies have been performed. They indicated that the present supramolecular polymer systems behave in a markedly different way compared with covalent polymers and display a very large drop in the standard viscosity with the applied shear; this may result from a mechanical stress-induced breaking of the

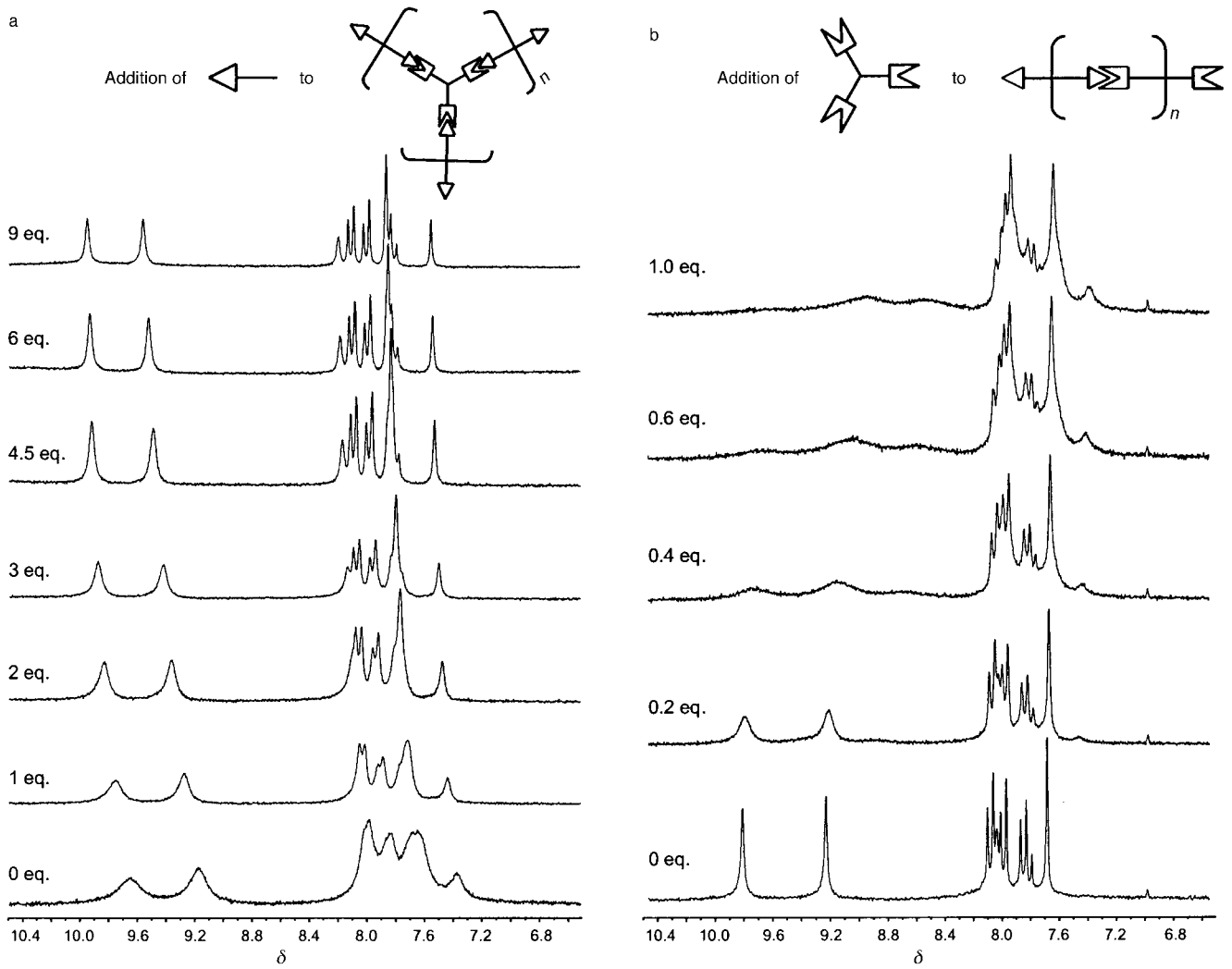

Figure 4. ^{1}H NMR spectra (200 MHz) of a) End-capping: addition of cyanurate **4** to $[\mathbf{2}:\mathbf{3}_{1.5}]_n$ (5 mM, $C_2D_2Cl_4$). b) Cross-linking: addition of trisreceptor **2** to cyanurate **4** to $[\mathbf{1}:\mathbf{3}]_n$ (2 mM, $C_2D_2Cl_4$). Monomer concentrations: **2**, 5 mM; **3**, 7.5 mM.

0947-6539/02/0805-1232 $ 17.50+.50/0 *Chem. Eur. J.* **2002**, *8*, No. 5

H-bonded aggregates. Related observations have been made on other systems.[23]

In the context of the dynamic nature of supramolecular polymers,[3, 9b] it is interesting to mention the observation of a rapid, reversible regeneration of the highly viscous aggregates under equilibrium conditions, after temporary destruction by the application of a high shear rate. These results, together with further work, will be described elsewhere.[46]

Crystal structure of bis-receptor 1: Numerous attempts were made to obtain single crystals suitable for X-ray analysis from both polymeric systems $[\mathbf{1}:\mathbf{3}]_n$ and $[\mathbf{2}:\mathbf{3}_{1.5}]_n$, and from the discrete entities $\mathbf{1}:\mathbf{4}_2$, $\mathbf{2}:\mathbf{4}_3$. A number of solvent combinations and diffusion techniques were tested, but they all led to precipitation of amorphous solids rather than to the formation of defined (co)crystals. However, slow diffusion of acetonitrile into a dilute (2.5 mM) solution of **1** in DMSO yielded single-crystalline needles which were analyzed by X-ray crystallography.

Figure 5a shows the tweezer-like structure of bis-receptor **1** in the crystal. The two planes of the isophthalic rings within one receptor molecule form an angle of 96.6°. The recognition groups show an interesting spatial arrangement. They are in the *s-cis*/*s-trans* conformation with respect to the aryl–CO bonds. This conformation is *not* the one suitable for binding a cyanuric substrate. Two intermolecular NH···O hydrogen bonds (3.05 Å, 165°) are formed from the terminal amide functionalities. There is no aromatic overlap between molecules of **1**, even though the representations may suggest it. Two molecules of DMSO per molecule of bis-receptor **1** are hydrogen bonded to the isophthalamides of the latter (NH···O: 2.86 Å, 171.6°) (Figure 5b). Thus, all the polar NH functions of bis-receptor **1** molecules are satisfied by hydrogen bonds, either with themselves or with solvent molecules.

These solid state features may be related to the solution state behavior of the bis-receptor **1** and of the trisreceptor **2**, in which conformational equilibria and intermolecular association by hydrogen bonding are presumably responsible for broadened proton NMR spectra and for the existence of discrete aggregates (as for pure receptor **1** in chloroform at temperatures below 40 °C). Similar behavior has been observed for a related isophthalamide molecular strand.[44]

Electron Microscopy studies: The addition of a hydrocarbon solvent such as heptane to stoichiometric mixtures of bis-receptor **1** and bis-wedge **3** (5–10 mM, chloroform) was found to result in a highly viscous mixture, the viscosity could be due to the formation of long and entangled fibers. Indeed, the

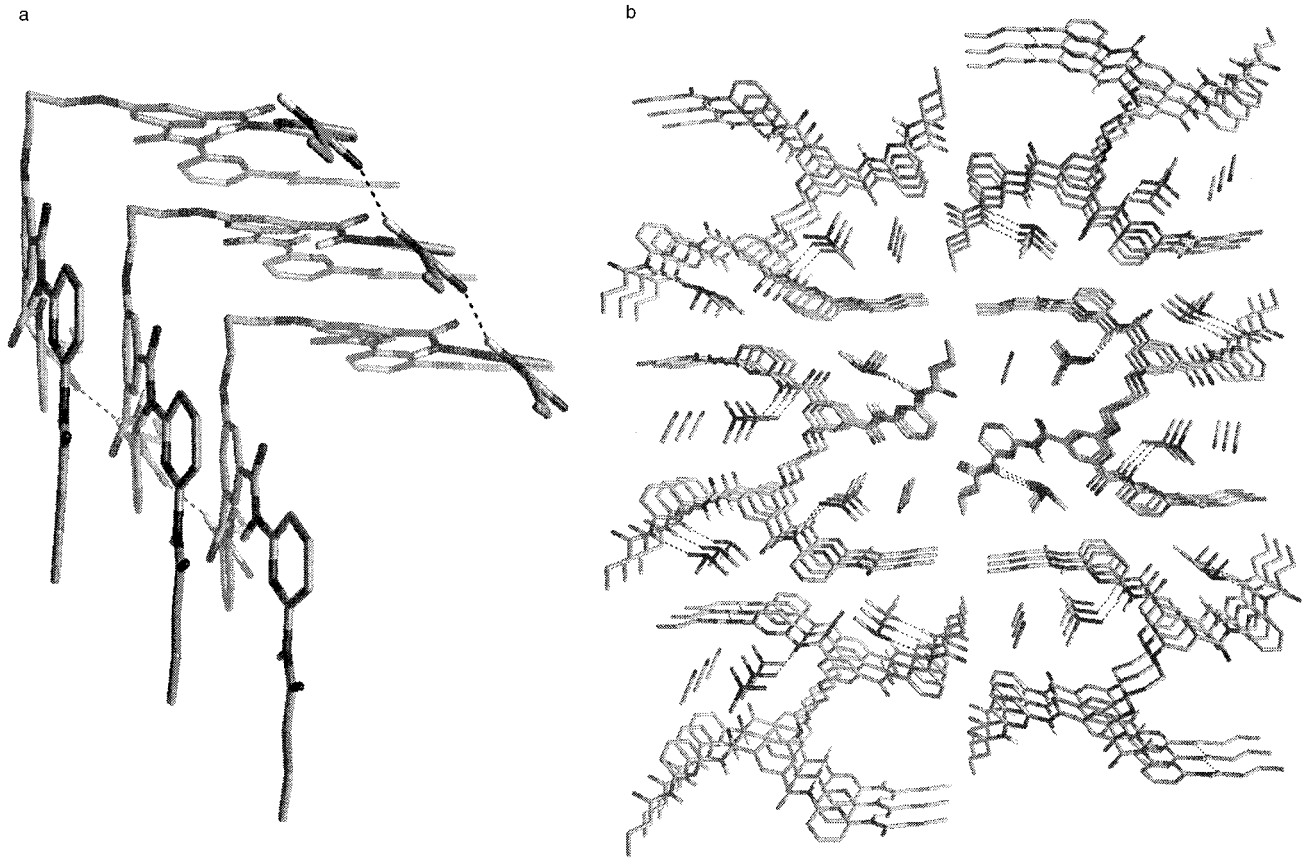

Figure 5. Stick representations of the crystal structure of bis-receptor **1**: a) side view of the relative arrangement of the tweezer-like structure, showing the intermolecular hydrogen bonds between terminal CO-NH amides as a black dotted line; b) top view of a crystal lattice intersection showing the DMSO molecules hydrogen bonded to the isophthalamide N*H*s. All C*H* hydrogens have been omitted for clarity. The structure has a monoclinic unit cell and contains 4 molecules of **1** (2 enantiomeric pairs), 4 molecules of MeCN, and 8 molecules of DMSO. The asymmetric unit cell only contains half a molecule of **1**, with the central methylene carbon of the propane bridge being part of a C_2-axis that generates the whole molecule by a 180° rotation.

decrease in polarity induced by the addition of the hydrocarbon solvent should enhance the strength of the hydrogen-bonded associations and lead to a shift in the species distributions toward higher-order polymeric assemblies. The solutions behave like reversible gels: they liquefy, that is loose their viscosity, upon heating and reform the gel after cooling and standing at room temperature. This interesting observation prompted the examination of these viscous solutions by electron microscopy (EM), which gave definitive evidence of aggregate formation.

Fiber formation in chloroform/heptane mixtures: That the viscous solutions indeed come from the formation of fibers was first indicated by EM studies on stoichiometric mixtures of bis-receptor **1** and bis-wedge **3** in chloroform/heptane (1:4, 2.5 mM). The viscous solutions were prepared by dissolving **1** and **3** in chloroform and adding excess heptane. The formation of fibers was detected by both direct observation and by cryofracture techniques. Figure 6 shows the extended fibrous networks observed in both cases. For comparative purposes, solutions of stoichiometric mixtures of **1** and **3** in pure chloroform (2.5 mM) were also investigated by EM, but no fibers or defined aggregates could be observed.

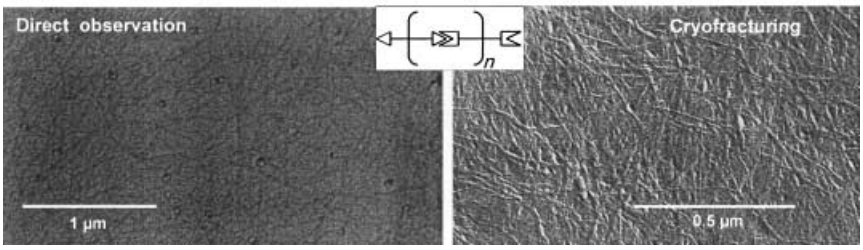

Figure 6. Extended, dense fiber network obtained from solutions of $[\mathbf{1}{:}\mathbf{3}]_n$ (2.5 mM) in $CHCl_3$/heptane (1:4) as evidenced by EM direct observation (left) and cryofracturing (right) techniques.

Fiber formation in tetrachloroethane: Tetrachloroethane was found to be a good solvent for observing fiber formation by EM investigations. Owing to its slower evaporation after placing a droplet of solution on the EM grid, the amount of deposited material could be more precisely controlled. A number of interesting observations were made.

All compounds, bis-receptor **1**, trisreceptor **2**, bis-wedge **3**, and mono-wedges **4** and **4b** dissolve readily in tetrachloroethane and remain in solution over time. When deposited on the EM grid as pure solutions in a concentration range from 1 to 10 mM, no trace of the formation of aggregates was observed. At most, unstructured material was deposited in an unspecific manner in these blank runs. However, when stoichiometric mixtures of **1** and **3** (2.5 to 10 mM with respect to each component) were used, the formation of well-defined helical fibers was observed (Figure 7).

The formation of fibrous aggregates from **1** and **3** was found to be critically dependent on the mode of mixture preparation. When solid mixtures of these two compounds were dissolved (after having weighed out the solids in the desired stoichiometric ratio in the same flasks), the formation of fibers was observed in all cases, as depicted in Figure 7. The solutions obtained from this simultaneous dissolution of **1** and **3** as solids in the same flask were perfectly translucent.

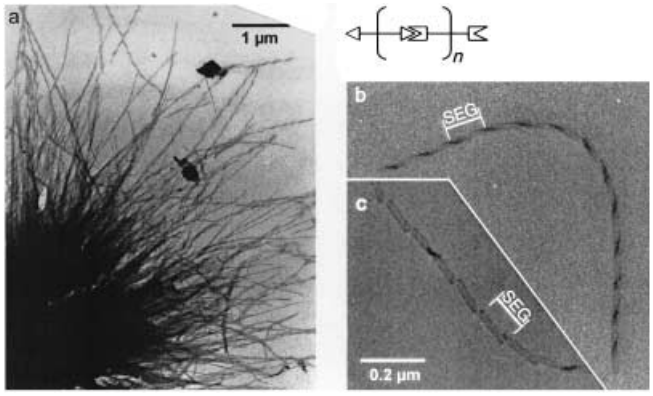

Figure 7. Helical fibers obtained from solutions of $[\mathbf{1}{:}\mathbf{3}]_n$ (5 mM) in $C_2H_2Cl_4$: a) helical fibers protruding radially from a dense tangle of material; b) enlargement of an isolated helical fiber showing the regular half-helical turns of 120 nm; c) breaking into rectangular rods of half a helical turn in length.

However, when the solutions were left standing for several hours at room temperature, a cloudiness appeared that further intensified upon standing over several additional days and resulted in a white "precipitate". This precipitate did not redissolve in tetrachloroethane, even when the suspension was sonicated for 24 h at 50 °C or heated under reflux at 146 °C. Only the addition of a polar (DMSO) or protic (methanol) solvent and subsequent heating to near reflux finally drove the redissolution of this solid, that indeed consisted of **1** and **3** (by NMR spectroscopy). A possible explanation for this observation could be the formation of a polymeric fibrous assembly on the basis of hydrogen bonds that precipitates out of the solution once a critical size is obtained, probably in the form of aggregated fibers. The aggregate only redissolves in the presence of a polar/protic solvent that competes with the hydrogen-bonding sites and disrupts the polymer. Such an irreversible supramolecular polymerization, as observed in tetrachloroethane, is reminiscent of the irreversible association of proteins in the brain to form protein aggregates, whose deposition is at the origin of neuro-degenerative diseases, such as Alzheimer's and Creutzfeldt–Jakob disease.[47]

Interestingly, very little fiber formation was observed when the solutions were prepared from separate stock solutions of the individual components. One possible explanation for these observations could be that the local concentration generated by the simultaneous dissolution of the solids is much higher at the solid–liquid interface during the dissolution process than in the mixing of two stock solutions. This could lead in one case to high molecular weight aggregates from the very start and drive the subsequent irreversible precipitation from the mixture with time, a trend not observed for the mixtures prepared from separate stock solutions.

On account of these observations, all samples subsequently studied in tetrachloroethane were prepared by directly dissolving the compounds as their solid mixtures. Neverthe-

  0947-6539/02/0805-1234 $ 17.50+.50/0 *Chem. Eur. J.* **2002**, *8*, No. 5

less, the results obtained from the EM observations of various samples were not perfectly reproducible in all the cases studied. However, the general trends and observations can be summarized as follows.

EM studies on stoichiometric mixtures of bis-receptor **1** *and bis-wedge* **3** *in* $C_2H_2Cl_4$: The predominant polymeric structures observed after the deposition of stoichiometric mixtures of **1** and **3** (2.5–10 mM) in tetrachloroethane are isolated helical fibers, found more or less homogeneously spread over the EM grid, and dense tangles of material, out of which a multitude of fibers grow radially. The fibers observed can be several micrometers long (Figure 7a) and exhibit a high persistence length. The individual fibers do not tend to aggregate into larger superstructures. The diameter of the twisted fibers varies from 100 to 200 Å; this suggests that they themselves constitute an aggregate of several polymeric threads, the relative positioning of which within the fiber cannot be resolved by EM. The formation of twisted ribbons is only observed for a certain fiber thickness (100–200 Å). If the diameter of the fibers exceeds this thickness, especially toward the interior of a dense tangle (Figure 7a), rod-like, uncoiled linear structures are observed.

Molecular modeling calculations suggest a length of about 45 Å for the linearly disposed repeating unit **1**:**3**, assuming a linear supramolecular polymerization mode, as depicted in Scheme 2. If these linear supramolecular threads constitute the macroscopically observed multimicrometer-sized fiber, this would correspond to the stringing together of several hundred of these units.

A characteristic property of these ribbon-like fibers is their internal helicity. In principle, a ribbon band has two possible ways of coiling into a helical superstructure, as depicted in Figure 8. A lateral twisting force conditions the formation of

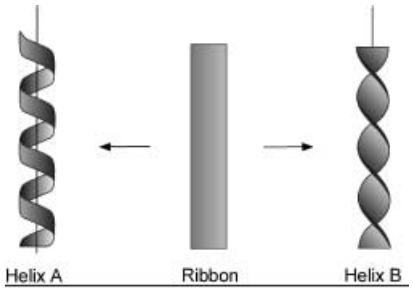

Figure 8. Generation of two types of helices from a flat ribbon precursor.

both helical type A and type B structures.[48] In the case of the twisted fibers formed by supramolecular polymer $[\mathbf{1}:\mathbf{3}]_n$, we exclusively observed the formation of helical type B structures. Both left- and right-handed helical twists were found when examining the EM pictures. Helical induction, or more precisely the transmission of molecular chirality onto a supramolecular level, from the enantiomerically pure tartaric bis-wedge **3** is apparently not strong enough to stabilize one macroscopic handedness with respect to the other. Thus, the macroscopic formation of chiral twisted-ribbon fibers is not a result of chiral amplification of the molecular chirality, as found earlier for triple helical supramolecular polymers.[13, 14] It may be due to a mode of association of the polymeric molecular strands within the fiber not having any preference for one or the other chirality. The half helical pitch is about 120 nm on average (Figure 7b); this would correspond to about 25 linearly disposed molecular repeat units **1**:**3**. Upon deposition of the helical fibers on the EM grid, a periodic breaking of the helical segments to form aligned elongated units of about 120 nm in length is often observed (Figure 7c). This periodic breaking could represent the persistence length of the fibers, but the experiments performed seem to indicate that it results rather from the operation of cohesion forces between the fiber and the EM grid surface; this reflects the preference for maximizing the surface contact with the object.

EM studies on the influence of an end-capping agent on mixtures of bis-receptor **1** *and bis-wedge* **3** *in* $C_2H_2Cl_4$: In order to investigate the structural effect of adding an end-capping agent, such as monotopic cyanurate **4** or barbiturate **4b**, on the fiber formation in tetrachloroethane, a series of samples of three-component mixtures of **1**, **3**, and **4** or **4b** were investigated (results not shown). The stoichiometries between the components were chosen so as to keep the total concentration of both receptor and substrate recognition groups constant (10 mM). The presence of substantial amounts of end-capping cyanurate **4** is required in order to observe noticeable changes in the aggregate formation. A significant destruction and shortening of the fibers can be noted at 0.3 equivalents of added **4**. Along with this observation, we noticed that less and less "structured" material was deposited on the grid with increasing amounts of end-capping agent. Compound **4b** seemed to have a stronger effect on the fiber destruction, which occurs at lower equivalent ratios (0.2 equiv) than with **4**. However, even if the presence of an end-capping agent has a clear effect on the structure, especially on the length of the fibers, the observations remain qualitative. For all equivalent ratios of end-capping agent investigated (up to 0.5 equiv), parts of the grids still contained the "regular", extended helical fibers as observed in the case of a simple 1:1 mixture of **1** and **3**.

Changing the stoichiometry (x and y) between the components in the system $[\mathbf{1}_x:\mathbf{3}_y]$ in both directions (at 5 mM initial concentration in tetrachloroethane) also resulted in a considerable shortening of the fibers. At $|x-y|>0.5$, most of the observable material is deposited in an unspecific manner (results not shown). No fibers could be found on the grids. Thus, the change in the stoichiometry has a similar effect as the addition of an end-capping agent in the three-component systems.

EM studies on the influence of a cross-linking agent on mixtures of bis-receptor **1** *and bis-wedge* **3** *in* $C_2H_2Cl_4$: The addition of small amounts of a branching agent, such as trisreceptor **2**, has a marked effect on the fibrous objects formed by bis-receptor **1** and bis-wedge **3** (Figure 9). Different solutions containing these components **1**, **3**, and **2** in various proportions were prepared (keeping the total concentration of the receptor and substrate recognition groups

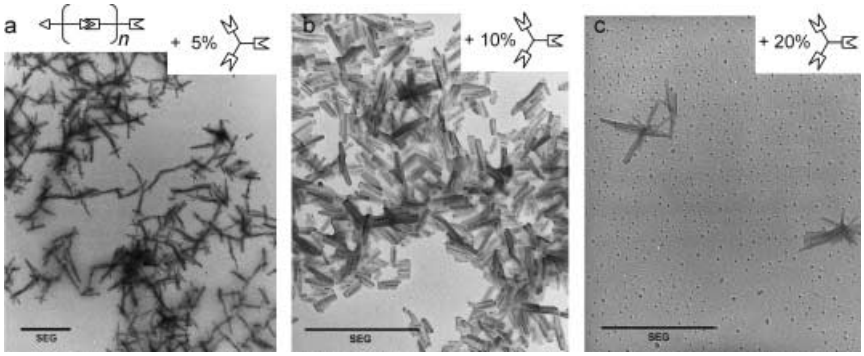

Figure 9. Electron microscopy studies revealing the strong influence of the addition of cross-linking agent **2** on the aggregate morphology of $[\mathbf{1}:\mathbf{3}]_n$ in $C_2H_2Cl_4$.

constant) and observed by EM. A mixture of **1**, **3**, and **2** in a 1:1.075:0.05 ratio (5% of branching agent) displays significantly shortened ($\ll 1$ μm) rod-like structures that no longer have helicity and seem to preferentially grow from specific centers in a star-shaped manner (Figure 9a). The objects formed by these three component mixtures shorten even more, when generated from a 1:1.15:0.1 ratio of the components. In this case, short rectangular blocks can be found either isolated or in the form of aggregates (Figure 9b). They do not exceed 500 nm in length and range from 30 to 50 nm in width. A further increase in the amount of branching agent to 20% results in the near disappearance of extended structures. Only isolated blocks are still observed (Figure 9c). For this percentage and also for higher percentages of branching agent (up to 40%), most material is deposited on the EM grid as circular "dots", in a very regular, uniform manner. These dots have a relatively narrow dispersity, with diameters ranging from 200 to 280 Å (Figure 9c).

These observations on the macroscopic objects can be reconciled with the postulated cross-linking of the molecular wires $[\mathbf{1}:\mathbf{3}]_n$ by **2**. The strong effect of **2** on the aggregate shape agrees with its incorporation into the polymeric edifice. The macroscopic outcome of the molecularly induced branching is not the formation of an entangled fibrous network. Instead, the molecular wires aggregate differently, showing a tendency to form closed objects. At a high molar ratio of **2** to **3**, the outcome of such an assembly would be nearly monodisperse "dots" instead of fibrous structures.

Fiber formation in toluene: Bis-receptor **1** and bis-wedge **3** are completely insoluble in toluene as individual compounds, given the polar and protic functions of the recognition groups of these molecules, which are poorly solvated by this apolar solvent. In contrast, their mixtures in about 1:1 stoichiometry dissolve readily in toluene. The main driving force is the H-bond complexation-induced solubilization of the polar recognition functions in the apolar solvent. The supramolecular polymer generated only exposes its lipophilic aromatic and aliphatic moieties to the solvent. In analogy to our observations in chloroform/heptane mixtures, the apolar solvent environment in toluene is expected to significantly increase the strength of the hydrogen-bonded associations, compared with chloroform or tetrachloroethane and lead to a shift in the species distributions toward higher-order polymeric assemblies. Indeed, highly viscous and visco-elastic solutions are formed for stoichiometric mixtures of **1** and **3** at initial concentrations above 2 mM. They behave like reversible gels.[46] These observations prompted investigations of these solutions by EM.

EM studies on the concentration dependence of fiber formation from stoichiometric mixtures of bis-receptor **1** *and bis-wedge* **3** *in toluene*: Interestingly, the solutions display a strong concentration dependence with respect to fiber formation, namely the length of the objects observed and their aggregation behavior on the EM grid (Figure 10).

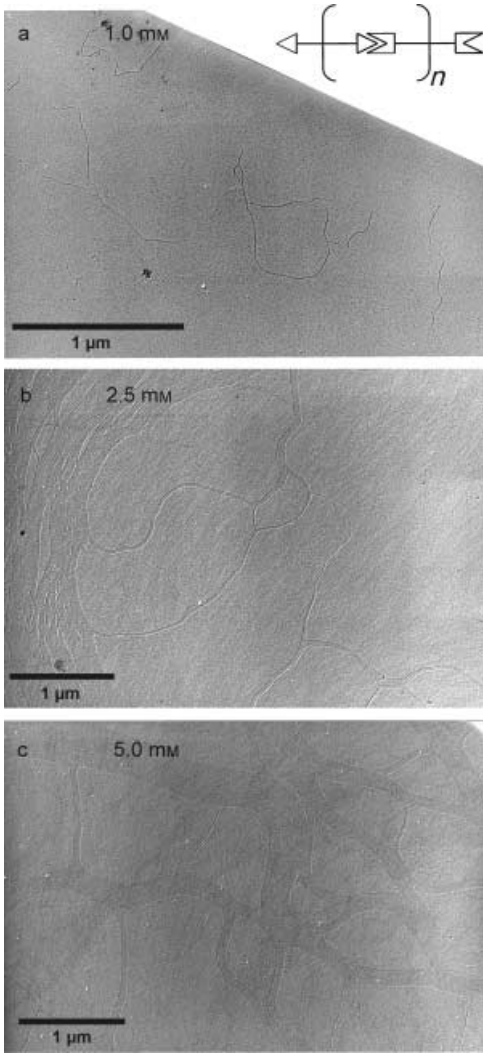

Figure 10. Electron microscopy studies on solutions of stoichiometric mixtures of bis-receptor **1** and bis-wedge **3** in toluene: a) 1 mM, short isolated fibers; b) 2.5 mM, isolated fibers and bundles; c) 5.0 mM, fibers and larger bundles.

0947-6539/02/0805-1236 $ 17.50+.50/0 *Chem. Eur. J.* **2002**, *8*, No. 5

1 mM solutions of the stoichiometric mixture of **1** and **3** in toluene resulted in the formation of thin (diameter < 120 Å) and relatively short fibers of less than 3 μm in length. The objects are randomly distributed on the EM grid and do not display internal helicity. Most fibers are open chain, but some closed circular structures are found as well. The fibers often show branching junctions; this indicates that they are themselves aggregates of several molecular threads. Compared with the straight helical fibers formed from tetrachloroethane solutions, the fibers from toluene do not have a high persistence length (Figure 10a).

Increasing the initial compound concentration to 2.5 mM yields fibers of much higher length, which tend to aggregate into bundles (Figure 10b). At 5 mM, we still see some isolated fibers, but the predominant motifs observed on the EM grid are wide (up to 0.5 μm in diameter), very thin bundles of fibers of *several dozens of μm* in length (Figure 10c). At 10 mM and above, the EM grid is uniformly coated with material (not shown).

The experiments support the expected increase in aggregate length with increasing concentration, and they show the interesting feature of a superimposed lateral-aggregation phenomenon of individual fibers to form larger flat cross-linked bundles on surfaces (see also Figure 3 in ref. [14]).

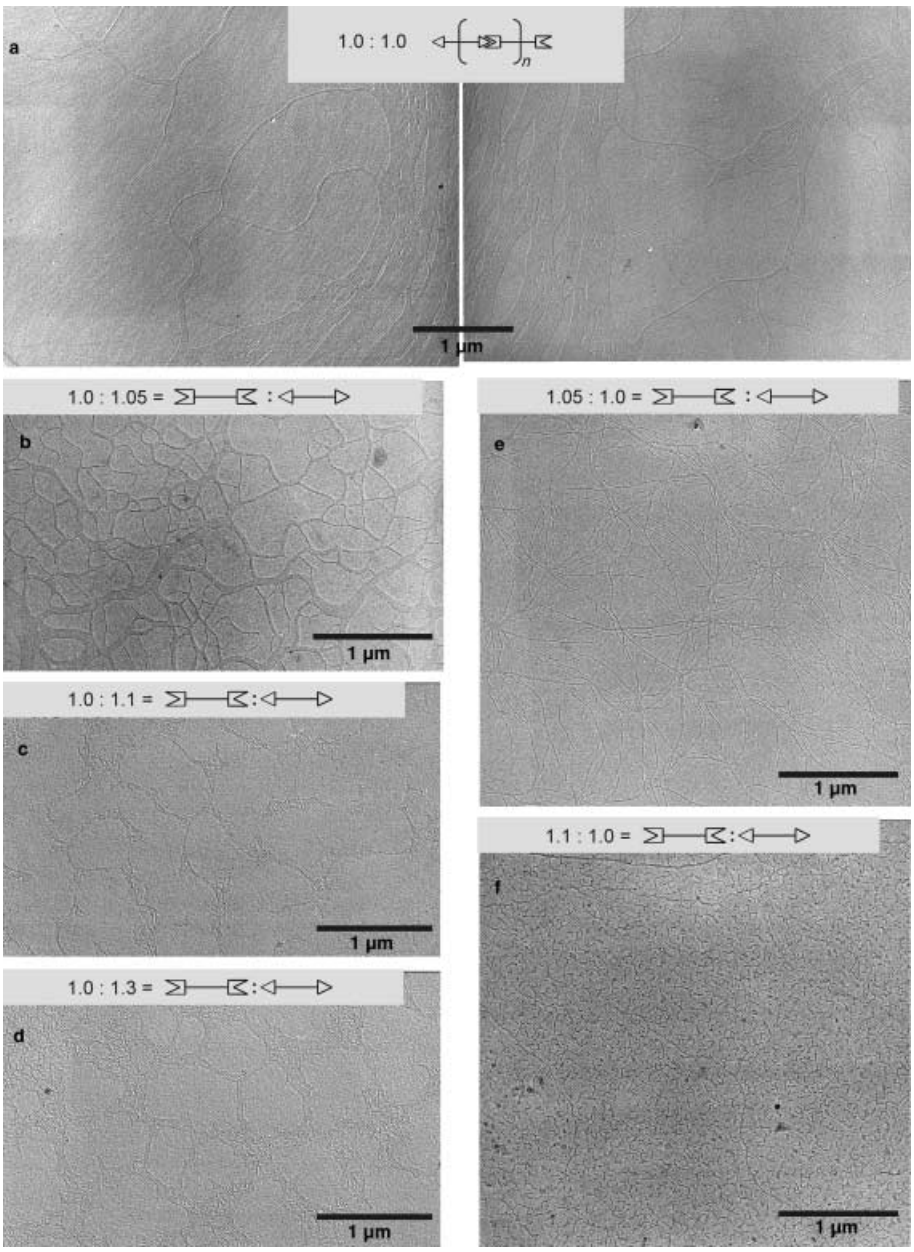

Figure 11. Electron Microscopy studies on the stoichiometry dependence of the shape of fibers formed from solutions of bis-receptor **1** and bis-wedge **3** in toluene (2.5 mM initial concentration): a) stoichiometric mixture of **1** and **3**; b)–d) stoichiometric imbalance in favor of **3**; e)–f) stoichiometric imbalance in favor of **1**.

EM studies on the influence of stoichiometry on the fibers formed from nonstoichiometric mixtures of bis-receptor **1** *and bis-wedge* **3** *in toluene*: Another set of experiments on the $[\mathbf{1}{:}\mathbf{3}]_n$ supramolecular polymer led to the demonstration of the strong dependency of fiber formation on the exact stoichiometry between the components (Figure 11). As little as a 5% difference with respect to exact stoichiometry in the two-component mixture has remarkable effects on the shape of the fiber in toluene.

If the $\mathbf{1}_x{:}\mathbf{3}_y$ stoichiometry is changed in favor of the bis-wedge **3** ($y > x$), there is a gradual destruction of the polymeric fibers initially present in the 1:1 mixture (Figure 11a). At a 1.0:1.05 ratio, we still observe long networked fibrous aggregates, but with the emergence of thin shortened branches (Figure 11b). In a 1.0:1.1 mixture, the destructive effect of the stoichiometric imbalance can be clearly seen. Long fibers and fiber bundles are still observed, but the amount of significantly shortened ones has considerably increased (Figure 11c). The fibers are markedly broken up into smaller units of less than 0.5 μm in length. The shortened fibers have a tendency to remain aggregated. The disintegration of the well-defined fibrous aggregates is even more pronounced if the stoichiometric ratio is changed to 1.0:1.3 (Figure 11d). Only randomly arranged regions of short thin fibers of less than 0.1 μm in length are observed, all the initially present long fibers having been destroyed. Most material is deposited in an undefined manner. A further increase in the stoichiometric imbalance to a 1.0:1.5 equiv-

alent ratio results in the deposition of unstructured material (not shown).

Upon changing the stoichiometry in the $\mathbf{1}_x$:$\mathbf{3}_y$ system in favor of bis-receptor **1** ($x > y$), a similar trend was observed. If mixed in a 1.05:1.0 equivalent ratio in toluene, the lateral aggregation of the fibers to form large bundles is much less pronounced. The only objects observed for this mixture are long (up to 10 μm) and thin (ca. 100–200 Å) fibrils (Figure 11e). However, in a 1.1:1.0 mixture, the destructive effect is remarkable. Although some longer (up to 4 μm) fibers are still present, the predominant objects found are considerably shortened (<0.1 μm) and quite uniformly distributed (Figure 11f).

These investigations of toluene solutions by EM corroborate the qualitative NMR observations and indicate a strong dependence of the supramolecular polymerization behavior of bis-receptor **1** and bis-wedge **3** on the stoichiometry of the compounds. The slight excess of one or the other component acts similarly to an end-capping agent on the dynamic supramolecular strand, significantly reducing its size. Thus, supramolecular polymers formed from heterocomplementary homoditopic monomers (**AA** and **BB**) represent "*self-capping*" systems, in which changes in stoichiometry of the two components allow manipulation of the degree of supramolecular polymerization.

The EM studies in toluene gave highly reproducible results. The type of objects formed were independent of sample preparation, and irreversible phenomena, for example precipitation (observed for the tetrachloroethane solutions), were not observed. The highly viscous solutions stayed perfectly translucid over time.

Comparison of the results from EM and the solution studies to a mathematical model: In order to correlate our experimental observations on the linear supramolecular polymer $\mathbf{1}_x$:$\mathbf{3}_y$ with a theoretical model, we developed a mathematical analysis for a linear **AA**-plus-**BB**-type supramolecular polymerization. Only self-complementary one-component **AB**-type supramolecular polymeric systems have yet been mathematically described.[23, 49] Statistical methods have been developed for describing the molecular weight distribution, the so called "most-probable" distribution, applicable to covalent step polymerization reactions, such as polycondensations.[50] We will see later that both approaches, our present thermodynamic approach to supramolecular polymers and Flory's statistical approach to describe covalent step-polymerizations, yield the same results.

The derivation of a mathematical model that simulates the behavior of homoditopic, two-component **AA**-plus-**BB**-type polymeric systems on the basis of the concentrations of and the association constants between the recognition groups involved should contribute to a better understanding of the observed characteristics of the linear supramolecular polymer $\mathbf{1}_x$:$\mathbf{3}_y$ (e.g. their highly concentration and stoichiometry dependent polymerization mode).[51]

In the present model of a linear **AA**-plus-**BB**-type supramolecular polymerization, we assumed the presence of the 2 species in solution, with a given initial concentration of c^0_{AA} and of c^0_{BB}, respectively, which assemble into linear supramolecular oligomers according to equilibria *i* (Table 1).

Table 1. First six equilibria between species **AA** and **BB**.

i	r_i	new species X_i	Constant	DP
1	1**AA** + 1**BB** ⇌	**AA**|**BB**	K	2
2	2**AA** + 1**BB** ⇌	**AA**|**BB**|**AA**	K^2	3
3	1**AA** + 2**BB** ⇌	**BB**|**AA**|**BB**	K^2	3
4	2**AA** + 2**BB** ⇌	**AA**|**BB**|**AA**|**BB**	K^3	4
5	3**AA** + 2**BB** ⇌	**AA**|**BB**|**AA**|**BB**|**AA**	K^4	5
6	2**AA** + 3**BB** ⇌	**BB**|**AA**|**BB**|**AA**|**BB**	K^4	5

r_i and s_i: stoichiometry coefficients; X_i: species formed; i: incremental number for indexed independent variables; K: association constant, DP: degree of polymerization.

Further assumptions include: a) a unique and known association constant K applicable to all equilibria (each consecutive binding step occurs with the same standard free energy change), b) the absence of any type of length effects (e.g. solubility, aggregation), and c) the absence of intramolecular associations (e.g. cyclization).

For every i, a general equilibrium equation can be written (concentration of species $X_i = c_i$):

$$K^{r_i + s_i - u_i} = \frac{c_i^{ti}}{\left(c^0_{AA} - \sum_{i=1}^{i_{max}} r_i \cdot c_i\right)^{r_i}} \cdot \left(c^0_{BB} - \sum_{i=1}^{i_{max}} s_i \cdot c_i\right)^{s_i}$$

Considering the boundary conditions (i + 2 independent variables, u_i being always 1), the following system of equations results:

i equilibria: $c_i \cdot c_{AA}^{-r_i} \cdot c_{BB}^{-s_i} - K^{r_i + s_i - 1} = 0$

2 boundary conditions: $c^0_{AA} - c_{AA} - \sum_{i=1}^{i_{max}} r_i \cdot c_i = 0$

$$c^0_{BB} - c_{BB} - \sum_{i=1}^{i_{max}} s_i \cdot c_i = 0$$

Simplification and solution of the above system of equations will be presented in detail elsewhere.[51]

Calculated results and comparison with the experimental observations on the linear supramolecular polymer $\mathbf{1}_x$:$\mathbf{3}_y$: All calculations were based on the assumption of a unique association constant, which was chosen to be 40000 L mol^{-1}, so as to correspond approximately to the stability constants experimentally determined in chloroform (see above). The concentrations chosen are indicated below in the graphs in Figure 12.

The growth mechanism of a linear multistage open association involving two heterocomplementary components **AA** and **BB** produces three types of supramolecular species (*S1*, *S2*, *S3*), depending on whether the degree of polymerization (DP) is even or odd:

DP even: *Species S1*: $(\mathbf{AA}\,|\,\mathbf{BB})_i$

DP odd: *Species S2*: $\mathbf{AA}\,|\,(\mathbf{BB}\,|\,\mathbf{AA})_j$ and
Species S3: $\mathbf{BB}\,|\,(\mathbf{AA}\,|\,\mathbf{BB})_j$

0947-6539/02/0805-1238 $ 17.50+.50/0 *Chem. Eur. J.* **2002**, *8*, No. 5

This is illustrated by the calculated number- and weight-fraction distributions. If the stoichiometry between **AA** and **BB** is the same, *S1* $(\mathbf{AA}\,|\,\mathbf{BB})_i$ are twice as abundant as *S2* $\mathbf{AA}\,|\,(\mathbf{BB}\,|\,\mathbf{AA})_j$ and *S3* $\mathbf{BB}\,|\,(\mathbf{AA}\,|\,\mathbf{BB})_j$, the last two having the same distribution (Figure 12a and b). Minor changes in the stoichiometry induce a strong imbalance in the relative occurrences of the species, all of which have now different distribution curves (Figure 12c and d).

The broad distributions obtained resemble the aforementioned "most probable" distribution known for step-growth covalent polymerizations, such as polycondensations.[51] In fact, they are identical. The concentration of oligomers decays monotonously with the number of their unimers, that is with the degree of polymerization (number-fraction distribution, Figure 12a and c). The weight-fraction distribution (Figure 12b and d), however, displays a maximum (DP_{max}) that is the same for the three species distributions. This maximum is commonly referred to as the number-average molecular weight (M_n).

The normalized weight-fraction distributions obtained by slight variations in the stoichiometry at constant total concentration reveal considerable shifts of the molecular-weight maxima to smaller values of DP_{max}. This indicates a strong influence of the stoichiometry on the average size of the aggregates obtained. Plotting the DP_{max} values (at a given constant total concentration) as a function of the mole fraction of either of the two compounds is an even better diagnostic for visualizing the amplitude of the effect of the stoichiometric imbalance in this two-component system (Figure 13). A very sharp distribution is obtained, showing the expected maximum for the stoichiometric mixture of the two compounds.

The results obtained enlighten, from a theoretical point of view, the experimental results from solution and EM studies on the linear supramolecular polymeric system $\mathbf{1}_x$:$\mathbf{3}_y$. The destructive effect of a stoichiometric imbalance on the fibers formed from solutions in toluene has been documented above by EM, supported by additional EM observations from solutions in tetrachloroethane and qualitative evidence from NMR solution studies.

As expected, the maxima of weight-fraction distributions (values of DP_{max}) obtained also depend critically on the total concentration in the two-component mixture. Figure 14a illustrates a shift toward higher degrees of polymerization with increasing concentration.

Similarly, Figure 14b shows the increase in the degree of supramolecular polymerization with increasing association constants between the recognition groups.

These results corroborate our experimental results on the supramolecular polymer $[\mathbf{1}:\mathbf{3}]_n$, which have revealed the strong concentration dependence of fiber formation (from 1 to 10 mM) in toluene as observed by EM. That the size of the aggregates obtained for $[\mathbf{1}:\mathbf{3}]_n$ also depends on the strength of the association, agrees with the results obtained on addition of hydrocarbon to chloroform solutions; this leads to an increase in stability constant between the hydrogen-bonded recognition groups as a result of the decrease in polarity of the solvent mixture.

The results obtained by the present mathematical model are in good agreement with the trends observed in solution

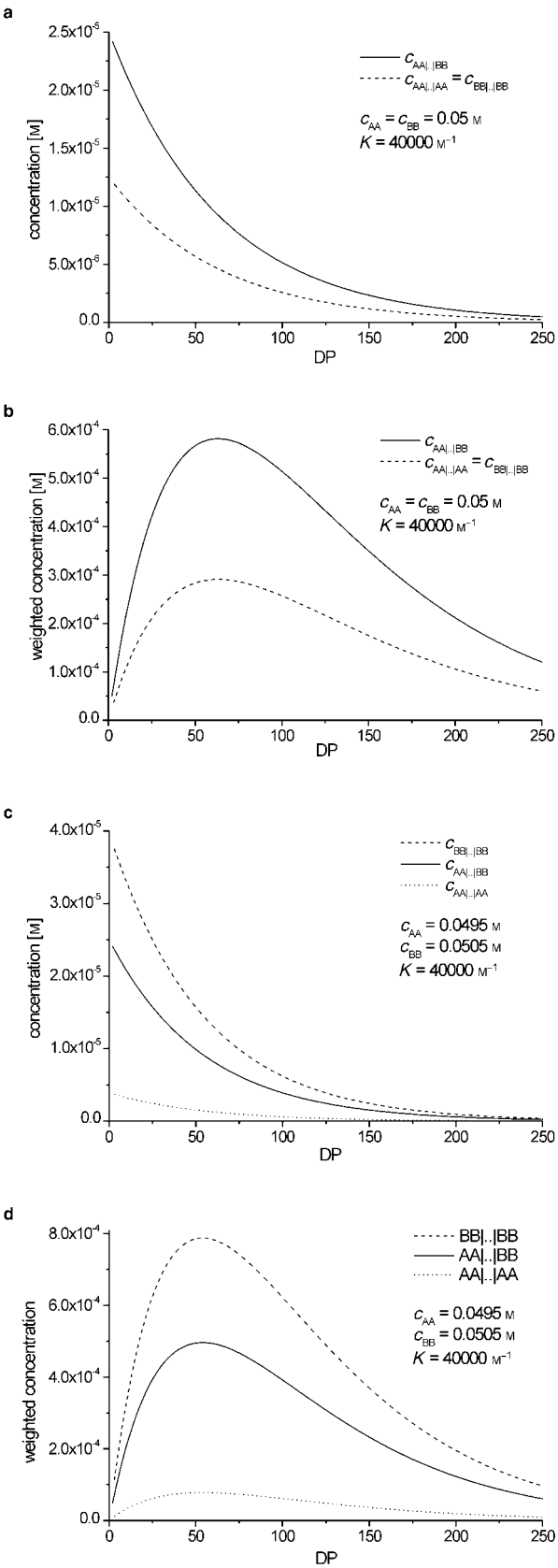

Figure 12. Calculated number-fraction distribution (a) and weight-fraction distribution (b) of an **AA**-plus-**BB**-type linear supramolecular polymer formed from stoichiometric amounts of monomers ($K = 40000$ L mol^{-1}, $c_{AA} = c_{BB} = 50$ mM). Calculated number- (c) and weight-fraction distribution (d) at a slight stoichiometric imbalance between **AA** and **BB** ($c_{AA} = 49.5$ mM; $c_{BB} = 50.5$ mM).

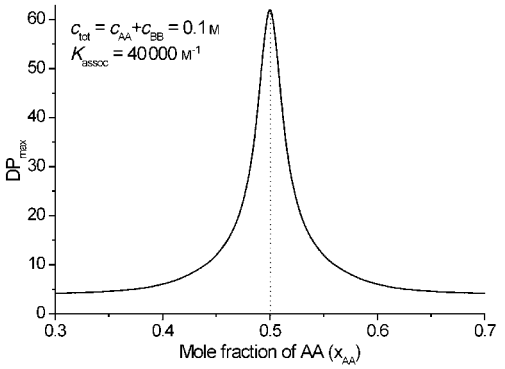

Figure 13. The consequences of stoichiometric imbalance on the extent of supramolecular **AA**-plus-**BB**-type polymerization: a) molecular-weight distributions obtained for different stoichiometric ratios at constant total concentration (100 mM, $K = 40000$ L mol^{-1}); b) the degree of polymerization (DP_{max}) as a function of the mole fraction of **AA**.

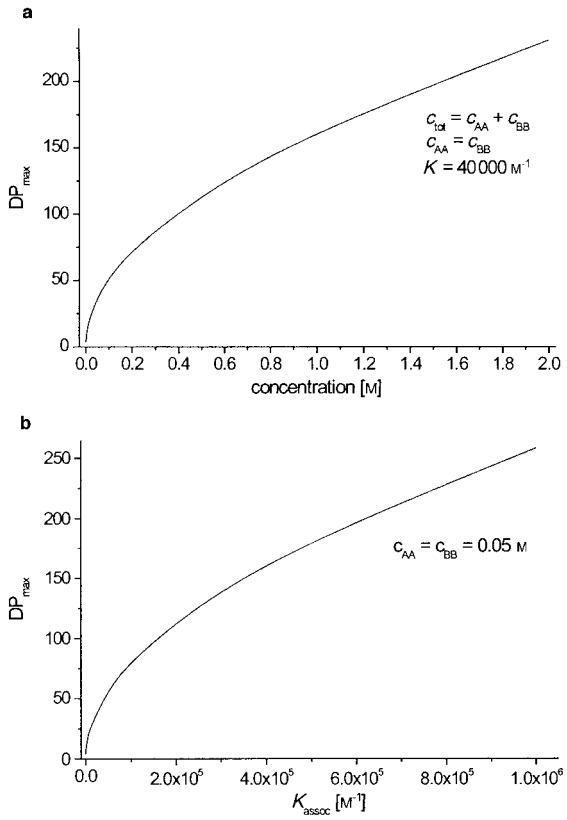

Figure 14. The degree of polymerization (DP_{max}) as a function of a) the total concentration and b) the strength of the association, for stoichiometric mixtures of compounds **AA** and **BB**.

and by EM. They support the concentration and stoichiometry dependence of a two-component homoditopic supramolecular polymeric system, which allows a certain level of control over the thermodynamically driven polymerization. They show the importance of a strong association constant between the recognition groups to achieve molecular-weight distributions with a weight-fraction maximum at high molecular weights.

It should be emphasized that the correspondence between the mathematical model and EM observations is *qualitative and only describes similar trends.* EM cryofracturing techniques have undoubtedly proven the existence of micrometer-sized fibrous objects in solution. However, the laterally aggregated large objects (with respect to molecular dimensions, that the EM cannot resolve), observed by EM in toluene solutions, may not be exactly the type of aggregates formed in these solutions. Surface forces and evaporation-induced concentration changes during the preparation of the EM grids for direct observation may drive the formation of these objects, and are, of course, not taken into account in a simplified thermodynamic treatment. Nevertheless, we would expect the model to be applicable to relatively dilute solutions, in chloroform for example, in which the extent of supramolecular polymerization is not expected to yield very high molecular weight fractions.

Conclusion

The present studies have analyzed the formation of the linear supramolecular polymers $[\mathbf{1}:\mathbf{3}]_n$ through molecular-recognition-induced self-assembly of two homoditopic monomeric components and their polyassociation into larger fibrous structures. These materials have revealed their dynamic nature, that is, their capacity to change the molecular-size distribution of their species, through their reversible adaptation to external factors such as concentration, temperature, solvent, and stoichiometry as well as the addition of cross-linking and end-capping agents. By this adaptive behavior, their properties can be reversibly tuned in a way not accessible to traditional covalent polymers. In toluene, the association is so strong, that even 1 mM solutions are highly viscous, which is a property similar to conventional polymers. Construction of such architectures requires sufficiently strong noncovalent interactions and eventually cooperativity effects in order to counter the increased entropic cost associated with the formation of highly ordered assemblies.

Thermodynamically controlled polymer formation implies several interesting aspects that could also be of industrial interest. For example, in coatings and hot melts, a reversible and strongly temperature-dependent viscosity is a much sought-after property. The supramolecular principles underlying the construction of these materials imply a continuous reorganization of their structure; this allows for self-repair and self-healing, unlike conventional polymers that permanently incorporate the defects of their formation.[2, 9b] Their reversible nature also confers on these entities the characteristics of "living" polymers.

Although several methods have been employed to characterize supramolecular polymers, it would be desirable to apply other physicochemical techniques in order to evaluate their features such as thermal and rheological behavior, mechanical properties, etc.

The observed thermal stability of the supramolecular polymeric aggregates formed under certain conditions (irreversible precipitation from tetrachloroethane at RT) is an interesting phenomenon with regard to two aspects. First, it suggests the suitability of the supramolecular approach toward functional and versatile materials that can, however,

  0947-6539/02/0805-1240 $ 17.50+.50/0 *Chem. Eur. J.* **2002**, *8*, No. 5

be more or less easily degraded to their molecular units by modifications of environmental conditions to the detriment of their stability, such as warming in the presence of a protic or polar solvent. On the other hand, the relation to irreversible polyaggregation and pathological material-deposition phenomena in biology suggests the need for a better understanding of the underlying processes involved.

Finally, structural modifications on both the recognition groups and the spacers that link them, as well as the effects of modifications in external factors and stimulations, must be investigated in order to further explore the novel properties offered by supramolecular polymers by virtue of their behavior as dynamic combinatorial materials and thus adaptive materials.[3, 9b, 10]

Experimental Section

General methods: THF was distilled over sodium/benzophenone. Triethylamine (Lancaster, 99%) was used as received. 2,6-Diaminopyridine (**6**; Aldrich, 98%) was purified by recrystallization from hot chloroform after filtration with charcoal (Norit A, < 100 mesh, Aldrich). All other commercially available products were used without further purification. Flash column chromatography was performed by using silica gel (Geduran, SI 60 (40–63 μm, Merck). Prior to the determination of stability constants, [D]chloroform was filtered over a short column of dry aluminium oxide 90. Infrared spectra were recorded as thin films on NaCl discs on a Perkin Elmer 1600 Series FTIR. The absorptions ($\tilde{\nu}$) are given in cm^{-1}. 500 MHz ^1H NMR spectra were recorded on a Bruker ARX 500 spectrometer, while 200 MHz ^1H NMR and 50 MHz ^{13}C NMR spectra were recorded on a Bruker SY 200 spectrometer. The solvent signal was used as an internal reference for both ^1H and ^{13}C NMR spectra. EI and FAB mass spectrometric measurements were performed by the Service de Spectrométrie de Masse, Institut de Chimie, Université Louis Pasteur. Melting points were recorded on a Koffler Heizblock apparatus and are uncorrected. Elemental analyses were performed by the Service de Microanalyse, Institut de Chimie, Université Louis Pasteur.

X-Ray crystallographic data for compound 1: Single crystals of **1** were obtained by slow liquid–liquid diffusion of MeCN into a solution of **1** in DMSO. As the crystals for compound **1** proved to be too small for analysis with conventional X-ray equipment, measurements were carried out at beamline ID11 at the European Synchrotron Radiation Facility (ESRF) at Grenoble. A wavelength of 0.5040 Å was selected by using a double-crystal Si(111) monochromator, and data were collected with a Bruker "Smart" CCD-camera system at fixed 2θ, while the sample was rotated over 0.1° intervals during 2 s exposures. Data were reduced with the Bruker SAINT software. Structure solution by direct methods and refinement on F^2 (using all independent data) by full-matrix least-square methods (SHELXTL 97). Hydrogen atoms were included at calculated positions by using a riding model. Details of the data collection and analysis are summarized in Table 2.

Crystallographic data (excluding structure factors) reported for **1** have been deposited with the Cambridge Crystallographic Data Centre as supplementary publication no. CCDC-172036. Copies of the data can be obtained free of charge on application to CCDC, 12 Union Road, Cambridge CB2 1EZ, UK (fax: (+44) 1223-336033, e-mail: deposit@ccdc.cam.ac.uk).

Electron Microscopy:

a) Direct observation: solutions of the compounds under investigation (1 to 10 mM) in different solvents (5 μL) were deposited onto a 400 mesh EM grid covered with a carbon supporting film. After 1 min, to allow for sample adsorption, the excess solution was removed with a piece of filter paper (Whatman 2 or 5), and the grids were air dried. They were then placed in an Edwards Auto 306 evaporator and rotary shadowed at an angle of 13° with platinum/tungsten. The grids were observed under a Philips CM12 electron microscope operating at 100 kV.

Table 2. Crystallographic parameters for the crystal structure determination of bis-receptor **1**.

molecular formula	$C_{55}H_{60}N_{12}O_{10}\cdot CH_3CN\cdot 2(C_2H_6SO)$
M_r [g mol^{-1}]	1246.37
crystallizing solvent/precipitant	DMSO/acetonitrile
crystal dimensions [mm]	$0.02\times 0.02\times 0.02$
color	colorless
T [K]	100(2)
λ [Å]	0.5166
crystal system	monoclinic
space group	$C2/c$
a [Å]	33.815(7)
b [Å]	4.975(1)
c [Å]	43.915(9)
$\alpha=\gamma$ [°]	90
β [°]	97.47(3)
volume [Å^3]	7326(3)
Z	4
ρ_{calcd} [g cm^{-3}]	1.132
F[000]	2640
scanned θ range [°]	0.68–19.22
index ranges	$-41=h=41$
	$-5=k=4$
	$-55=l=54$
reflections collected	28036
R(int)	0.0627
independent reflexions	5899
data/restraints/parameters	5899/0/463
GoF	1.016
final R indices [$I>2\sigma(I)$]	$R_1=0.0614$
	$wR_2=0.1783$
R indices (all data)	$R_1=0.0735$
	$wR_2=0.1901$
resid. e$^-$ density [e Å^{-3}]	1.132

b) Cryofracturing: A drop of the gel was sandwiched between two copper specimen holders and plunged in liquid nitrogen before being transferred into the cryofracture device (developed at IGBMC by J.-C. Homo). The specimen holder was kept at $\sim 10^{-8}$ torr and −178 °C. The vitrified sample was fractured, followed immediately by shadowing at 45° with Pt/C (20 Å thickness as measured with a quartz crystal) and reinforced with 200 Å carbon at normal incidence. The replicas were washed in chloroform, retrieved with a 400 mesh copper grid covered with a carbon supporting film, and observed again with a Philips CM12 electron microscope operating at 100 kV.

NMR relaxation times: determination and analysis: The relaxation times of protons, including H_B (Figure 15), were determined by standard inversion–recovery experiments and subsequent exponential curve fitting. For their analysis we assumed that relaxation takes place exclusively by intramolecular dipole–dipole relaxation modes, neglected other possible relaxation contributions (the presence of oxygen in the solutions, the intermolecular relaxation modes, and the chemical shift anisotropy), and used a 10% experimental error range. We could then plot, at both 200 MHz and 500 MHz, for each proton signal whose T_1 was *experimentally* determined, the *calculated* evolution of its relaxation time as a function of the rotational-diffusion correlation time τ. This is achieved by using Equation (1)[52, 53] and distances between the neighboring hydrogens as determined by molecular modeling (energy minimization with *Macro-Model*, version 6.5, Amber force field).

$$\frac{1}{T_1}=\sum_{i=1}^{n}\frac{3}{10}\frac{\gamma_H^4\hbar^2}{r^6}\left(\frac{\tau_c}{1+\omega_0^2\tau_c^2}+\frac{4\cdot\tau_c}{1+4\cdot\omega_0^2\tau_c^2}\right)\ \text{(variables in cgs units)}\quad(1)$$

$\omega_0=2\pi\nu_0$, $\nu_0=$ spectrometer frequency [Hz], $\gamma_H=$ gyromagnetic constant for hydrogen, $\tau_c=$ correlation time, $r=$ distance between proximal hydrogens, and $i=$ number of proximal hydrogens.

The positioning of the four experimentally determined values of T_1 for selected protons in the discrete complex **1**:**4**$_2$ and in the supramolecular polymer [**1**:**3**]$_n$ on their corresponding calculated relaxation time curves, at 200 and 500 MHz, results in a significant increase in the correlation time of

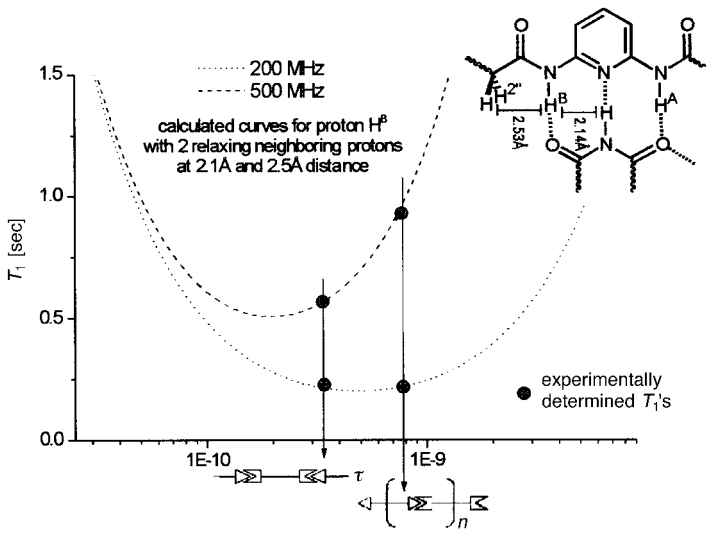

Figure 15. Evolution of the calculated relaxation time T_1 of proton H_B as a function of the rotational diffusion correlation time τ_c, and positioning of the experimentally determined relaxation times on the curves (●).

the supramolecular polymer $[\mathbf{1}{:}\mathbf{3}]_n$ at the high spectrometer frequencies. This is in agreement with the assumed presence of higher-molecular-weight material in solution for the $[\mathbf{1}{:}\mathbf{3}]_n$ polymer compared with the discrete complex $\mathbf{1}{:}\mathbf{4}_2$. Figure 15 illustrates these findings by using the results obtained for proton H_B (τ ($[\mathbf{1}{:}\mathbf{3}]_n$) $= 7.94 \times 10^{-10}$ s and τ ($\mathbf{1}{:}\mathbf{4}_2$) $= 2.63 \times 10^{-10}$ s).

If other proton signals are followed, the values of τ can be markedly different; this suggests that our model has limitations with respect to its accuracy or that the different protons may be subject to additional modes of relaxation that have been neglected for simplicity reasons.

By further evaluation of the relaxation time results, it is possible to evaluate a rough molecular volume V_m for the polymer $[\mathbf{1}{:}\mathbf{3}]_n$ on the basis of Equations (2). It was assumed that the viscosity of chloroform is not considerably affected under these conditions (initial concentration of **1** and **3**: 10 mM) ($\eta_{CHCl_3}(25\,^\circ C) = 0.537$ mPa s).

$$V_m = \frac{\tau_c kT}{\eta} \quad \text{with} \quad \tau_c = \frac{4\pi\eta a^3}{3kT} \tag{2}$$

With the observed value of $\tau_{max} = 8 \times 10^{-10}$ s, the molecular volume of the $[\mathbf{1}{:}\mathbf{3}]_n$ aggregate was calculated to be approximately 6000 Å^3. In order to determine to which average polymerization extent this value corresponds, molecular volume calculations were carried out with the program *Spartan* (Version 5.1.3, 1998, Wavefunction, Inc.). The volumes of a molecule of bis-receptor **1** and bis-wedge **3** were found to be approximately 1140 Å^3 and 860 Å^3, respectively. The molecular volume calculated by the relaxation data would thus correspond to an average trimeric aggregate $[\mathbf{1}{:}\mathbf{3}]_3$.

The change in the sign of the NOE cross peaks, observed between the imide NH of **3** and the amides of **1** for polymer $[\mathbf{1}{:}\mathbf{3}]_n$, with temperature (from 0 °C to 50 °C, 10 mM, $CDCl_3$) is also a qualitative indication of the passage from aggregated higher-molecular-weight supermolecules to low-molecular-weight species. As expected, the temperature increase is accompanied by a decrease in complex stability and a rupture of the polymeric H-bonded linear aggregates.

Synthetic procedures: 1,3,5-Tris(bromomethyl)benzene (**7**),[54] 1-decyl-[1,3,5]-triazinane-2,4,6-trione (**4**),[44] L-2,3-*O*,*O*-bis-dodecyl tartaric acid bis-[2-(2,4,6-trioxo-[1,3,5]-triazinan-1-yl)ethyl] ester (**3**)[40] were prepared according to procedures developed in other work. Receptor **13** and dihexadecyl barbiturate **4b** are described in refs. [55] and [56], respectively.

***N*-(6-aminopyridin-2-yl)-butyramide (8)**: 2,6-Diaminopyridine (**6**; 13.0 g, 119 mmol, 100 mol %) and triethylamine (12.7 g, 119 mmol, 100 mol %) were dissolved in dry THF (200 mL), and the solution was cooled to 0 °C in an ice bath. A solution of butyryl chloride (12.7 g, 125 mmol, 105 mol %) in THF (20 mL) was added dropwise over a period of 1 h, and the reaction was allowed to proceed at 0 °C for another 3 h, before warming to RT. The reaction mixture was filtered, evaporated to dryness and purified by chromatography (SiO_2, EtOAc/hexane 60:40). Compound **8** was obtained as a white powder. Yield: 12.8 g (60 %); m.p. 154–155 °C; IR (thin film): $\tilde{\nu} = 3326$, 3205, 1672, 1620, 1537, 1455, 1294, 1162, 794 cm^{-1}; ^{1}H NMR (200 MHz, [D$_6$]DMSO): $\delta = 9.74$ (s, 1H), 7.28 (m, 2H), 6.17 (d, $^3J = 7.2$ Hz, 1H), 5.67 (br s, 2H), 2.30 (t, $^3J = 7.1$ Hz, 2H), 1.56 (m, 2H), 0.86 (t, $^3J = 7.2$ Hz, 3H); ^{13}C NMR (50 MHz, [D$_6$]DMSO): $\delta = 171.6$, 158.4, 150.5, 138.7, 103.2, 101.0, 38.1, 18.5, 13.5; FAB-MS: *m*/*z*: 180.1 ([*M*+H]$^+$, 100 %); elemental analysis calcd (%) for $C_9H_{13}N_3O$ (179.22): C 60.32, H 7.31, N 23.45; found: C 60.09, H 7.57, N 23.39.

1,3-Bis-[3,5-bis(methoxycarbonyl)phenoxy]propane (9): (see also ref. [57].) A mixture of dimethyl 5-hydroxyisophthalate (**5**; 4.8 g, 23.1 mmol, 230 mol %), 1,3-dibromopropane (2.0 g, 10 mmol, 100 mol %), and K_2CO_3 (5.0 g, 36 mmol) in dry DMF (25 mL) was stirred at 60 °C for 45 h. The reaction mixture was poured into 800 mL of water, and the precipitate was collected by filtration. The solid was dissolved in CH_2Cl_2, washed once with 5 % aqueous NaOH, dried over Na_2SO_4, and evaporated to dryness. The residue was crystallized from CH_2Cl_2/hexane and dried under vacuum to afford **9** as a white solid. Yield: 3.7 g (80 %); m.p. 117–118 °C; IR (thin film): $\tilde{\nu} = 2953$, 1724, 1594, 1434, 1430, 1313, 1189, 1118, 1102, 1061, 1003, 908, 881, 756, 721 cm^{-1}; ^{1}H NMR (200 MHz, [D]chloroform): $\delta = 8.28$ (t, $^4J = 1.5$ Hz, 2H), 7.76 (d, $^4J = 1.5$ Hz, 4H), 4.27 (t, $^3J = 6.0$ Hz, 4H), 3.94 (s, 12H), 2.32 (m, 2H); ^{13}C NMR (50 MHz, [D]chloroform): $\delta = 166.1$, 158.9, 131.9, 123.2, 119.8, 64.8, 52.5, 29.1; EI-MS: *m*/*z*: 460.0 ([*M*]$^+$, 70 %); elemental analysis calcd (%) for $C_{23}H_{24}O_{10}$ (460.43): C 60.00, H 5.25; found: C 59.89, H 5.43.

1,3-Bis-[3,5-bis(carboxy)phenoxy]propane (10): Tetraester (**9**; 5.62 g, 12.2 mmol, 100 mol %) was suspended in 95 % aqueous ethanol (122 mL) and was warmed to 65 °C, at which time a solution of NaOH (2.92 g, 600 mol %) in water (12 mL) was added. After being stirred for 12 h at 65 °C, the mixture was allowed to cool before being filtered. The white precipitate was collected, washed once with cold ethanol (100 mL), and then dissolved in water (300 mL). This solution was filtered and treated with conc. HCl (6 mL). The precipitate was collected by filtration, washed with water, and dried under reduced pressure to afford title compound **10** as a white powder. Yield: 4.7 g (95 %); m.p. >260 °C; IR (thin film): $\tilde{\nu} =$ 3066, 1694, 1594, 1462, 1420, 1397, 1265, 1211, 1125, 1058, 882, 759, 724, 665 cm^{-1}; ^{1}H NMR (200 MHz, [D$_6$]DMSO): $\delta = 8.07$ (t, $^4J = 1.4$ Hz, 2H), 7.67 (d, $^4J = 1.4$ Hz, 4H), 4.27 (t, $^3J = 6.0$ Hz, 4H), 2.24 (m, 2H); ^{13}C NMR (50 MHz, [D$_6$]DMSO): $\delta = 166.3$, 158.6, 132.6, 122.3, 119.1, 64.8, 28.4; FAB-MS: *m*/*z* 403.2 ([*M* − H]$^-$, 100 %); elemental analysis calcd (%) for $C_{19}H_{16}O_{10}$ (404.32): C 56.44, H 3.99; found: C 56.56, H 3.94.

1,3-Bis-{3,5-bis-[6-(butyrylamino)pyridin-2-ylcarbamoyl]phenoxy}propane (1): Tetraacid **10** (0.90 g, 2.2 mmol, 100 mol %) was suspended in $SOCl_2$ (20 mL). A drop of dry DMF was added, and the solution was heated to reflux. After 20 min, the solid had entirely dissolved, and the solution was refluxed for a further 14 h. The excess $SOCl_2$ was distilled off, and the oily residue was kept under high vacuum for 30 min to afford the crude tetraacid chloride **10b**, which was used without further purification. Compound **10b** was dissolved in THF (5 mL) and cannulated into a previously prepared solution of **8** (1.68 g, 9.4 mmol, 420 mol %) and triethylamine (0.95 g, 9.4 mmol, 420 mol %) in THF (20 mL) at RT. The reaction was allowed to proceed for 1 h, after which time the reaction mixture was filtered, evaporated to dryness, and chromatographed (SiO_2, gradient: THF/hexane 50:50 → 80:20). Compound **1** was obtained as a slightly gray powder. Yield: 2.33 g (99 %), m.p. 155–160 °C; IR (thin film): $\tilde{\nu} = 3298$, 2952, 1689, 1640, 1584, 1504, 1446, 1292, 1242, 1156, 1071, 797 cm^{-1}; ^{1}H NMR (200 MHz, [D$_6$]DMSO): $\delta = 10.46$ (s, 4H), 10.05 (s, 4H), 8.15 (s, 2H), 7.80 (m, 16H), 4.38 (br t, $^3J = 5.8$ Hz, 4H), 2.38 (t, $^3J = 7.3$ Hz, 8H), 2.32 (br m, 2H), 1.61 (m, 8H), 0.90 (t, $^3J = 7.3$ Hz, 12H); ^{13}C NMR (50 MHz, [D$_6$]DMSO): $\delta = 172.0$, 164.8, 158.4, 150.5, 150.0, 139.9, 135.6, 119.7, 110.4, 109.9, 64.8, 37.9, 30.5, 18.3, 13.4; FAB-MS: *m*/*z*: 1049.4 ([*M*]$^+$, 100 %); elemental analysis calcd (%) for $C_{55}H_{60}N_{12}O_{10}$ (1049.14): C 62.96, H 5.76, N 16.02; found: C 62.89, H 5.99, N 15.88.

1,3,5-Tris-[3,5-bis(methoxycarbonyl)phenoxymethyl]benzene (11): A mixture of 1,3,5-tris(bromomethyl)benzene **7** (1.0 g, 2.8 mmol, 100 mol %) and K_2CO_3 (3.5 g, 25.5 mmol) in dry DMF (20 mL) was degassed with argon for 20 min. Dimethyl 5-hydroxyisophthalate (**5**; 2.0 g, 9.5 mmol, 330 mol %) in dry DMF (5 mL) was added dropwise, and the mixture was stirred at 65 °C for 28 h, after which time the reaction mixture was poured into 100 mL of ice/water. The aqueous phase was extracted with toluene (3 × 50 mL), and

  0947-6539/02/0805-1242 $ 17.50+.50/0 *Chem. Eur. J.* **2002**, *8*, No. 5

the combined organic fractions were washed with water (2×50 mL), dried over $MgSO_4$, and evaporated to dryness. The brown oily residue was purified by column chromatography (SiO_2, gradient: $CHCl_3 \rightarrow 10\%$ EtOAc/$CHCl_3$) to afford **11** as a white solid. Yield: 1.24 g (59%); m.p. 178–179 °C; IR (thin film): $\tilde{\nu} = 2954$, 1728, 1597, 1434, 1342, 1313, 1249, 1119, 1070, 1007, 909, 878, 845, 793, 722, 666 cm^{-1}; ^1H NMR (200 MHz, [D]chloroform): $\delta = 8.28$ (d, $^4J = 1.4$ Hz, 3H), 7.82 (d, $^4J = 1.4$ Hz, 6H), 7.51 (s, 3H), 5.16 (s, 6H), 3.92 (s, 18H); ^{13}C NMR (50 MHz, [D]chloroform): $\delta = 166.0$, 158.6, 137.3, 131.9, 126.2, 123.4, 120.0, 69.9, 52.4; FAB-MS: m/z: 745.2 ($[M+H]^+$, 82%); elemental analysis calcd (%) for $C_{39}H_{36}O_{15}$ (744.69): C 62.90, H 4.87; found: C 62.88, H 4.93.

1,3,5-Tris-[3,5-(dicarboxy)phenoxymethyl]benzene (12): A solution of $LiOH \cdot H_2O$ (0.46 g, 11.0 mmol, 700 mol%) in water (65 mL) was added to a stirred solution of **11** (1.17 g, 1.57 mmol, 100 mol%) in THF (75 mL), and the mixture heated to reflux for 6 h. Subsequently, the reaction was cooled to RT, EtOAc (50 mL) was added, and the aqueous layer was isolated. After dilution to 200 mL, the mixture was acidified with conc. HCl. The white precipitate **12** was filtered off, washed with water, ethanol and ether, and dried under high vacuum. Yield: 0.92 g (89%); m.p. >260 °C; IR (thin film): $\tilde{\nu} = 3004$, 2895, 1715, 1598, 1415, 1283, 1072, 879, 758, 741, 689 cm^{-1}; ^1H NMR (200 MHz, [D_6]DMSO): $\delta = 8.11$ (s, 3H), 7.77 (s, 6H), 7.62 (s, 3H), 5.29 (s, 6H); ^{13}C NMR (50 MHz, [D_6]DMSO): $\delta =$ 166.3, 158.4, 137.1, 132.6, 126.4, 122.5, 119.4, 69.5; FAB-MS: m/z: 659.1 ($[M-H]^-$, 51%); elemental analysis calcd (%) for $C_{33}H_{24}O_{15}$ (660.53) · $[H_2O]_2$: C 58.41, H 3.86; found: C 58.60, H 4.15.

1,3,5-Tris-{3,5-bis-[6-(butyrylamino)pyridin-2-ylcarbamoyl]phenoxymethyl}benzene (2): Hexaacid **12** (0.5 g, 0.77 mmol, 100 mol%) was finely pulverized in a mortar and suspended in $SOCl_2$ (60 mL). Five drops of dry DMF were added, and the solution heated to reflux. After 1.5 h, the solid had almost entirely dissolved, and the solution was refluxed for a further 18 h. The excess $SOCl_2$ was distilled off, and the oily residue was kept under high vacuum for 30 min to remove all acid traces. The crude hexaacid chloride **12b** was used without further purification. It was dissolved in dry THF (50 mL) and cannulated into a previously prepared solution of **8** (0.86 g, 4.8 mmol, 630 mol%) and triethylamine (0.50 g, 4.9 mmol, 650 mol%) in THF (20 mL). The reaction was allowed to proceed for 10 min at RT, after which time it was heated to 60 °C for 1 h. Methanol was added until the residual solids from the mixture had completely dissolved, SiO_2 was then added, and the mixture was evaporated to dryness in preparation for a column (SiO_2, gradient: $CHCl_3$/EtOAc 40:60 $\rightarrow$ $CHCl_3$/EtOAc/EtOH 40:55:5). Compound **2** was obtained as a gray powder. Yield: 1.08 g (87%); m.p. 180–185 °C; IR (thin film): $\tilde{\nu} = 3288$, 2963, 2873, 1674, 1585, 1514, 1447, 1297, 1242, 1156, 1055, 876, 800, 748 cm^{-1}; ^1H NMR (200 MHz, [D_6]DMSO): $\delta = 10.49$ (s, 6H), 10.06 (s, 6H), 8.19 (s, 3H), 7.84 (m, 24H), 7.68 (s, 3H), 5.40 (s, 6H), 2.37 (t, $^3J = 7.2$ Hz, 12H), 1.60 (m, 12H), 0.90 (t, $^3J = 7.3$ Hz, 18H); ^{13}C NMR (50 MHz, [D_6]DMSO): $\delta =$ 172.0, 164.8, 158.4, 150.5, 150.0, 140.0, 137.4, 135.6, 126.4, 120.0, 117.6, 110.4, 110.0, 69.6, 38.0, 18.4, 13.5; FAB-MS: m/z 1627.5 ($[M]^+$, 100%); elemental analysis calcd (%) for $C_{87}H_{90}N_{18}O_{15}$ (1627.76): C 64.19, H 5.57, N 15.49; found: C 64.11, H 5.67, N 15.23.

Acknowledgement

This work was supported by the CNRS and by a predoctoral fellowship (V.B.) from the Forschungszentrum Karlsruhe GmbH and a post-doctoral NIH fellowship (R.G.K.). M.S. is supported by the INSERM, the CNRS and the CHU de Strasbourg. We thank Prof. E. Tsitsihvili for her assistance in establishing the thermodynamic mathematical model for the supramolecular two-component polymerization[51] as well as Victoria Ullery and Françoise Candau for preliminary viscosity and rheological measurements.[46]

[1] J.-M. Lehn, *Supramolecular Chemistry—Concepts and Perspectives*, VCH, Weinheim, **1995**, Chapter 9.
[2] J.-M. Lehn, *Macromol. Chem. Macromol. Symp.* **1993**, *69*, 1.
[3] J.-M. Lehn in *Supramolecular Science: Where It Is and Where It Is Going?* (Eds.: R. Ungaro, E. Dalcanale), Kluwer, Dordrecht, **1999**, p. 287 and Figure 4.
[4] R. F. M. Lange, M. van Gurp, E. W. Meijer, *J. Polym. Sci. Polym. Chem. Ed.* **1999**, *37*, 3657.
[5] J. S. Moore, *Curr. Opin. Colloid Interf. Sci.* **1999**, *4*, 108.
[6] N. Zimmerman, J. S. Moore, S. C. Zimmerman, *Chem. Ind.* **1998**, 604.
[7] R. P. Sijbesma, E. W. Meijer, *Curr. Opin. Colloid Interf. Sci.* **1999**, *4*, 24.
[8] C. T. Imrie, *Trends Polym. Sci.* **1995**, *3*, 22.
[9] a) *Supramolecular Polymers* (Ed.: A. Cifferi), Marcel Dekker, New York, **2000**; b) J.-M. Lehn, *Supramolecular Polymers* (Ed.: A. Cifferi), Marcel Dekker, New York, **2000**, pp. 615–641.
[10] J.-M. Lehn, *Chem. Eur. J.* **1999**, *5*, 2455.
[11] M. J. Krische, J.-M. Lehn, *Struct. Bonding* **2000**, *96*, 3.
[12] M.-J. Brienne, J. Gabard, J.-M. Lehn, I. Stibor, *J. Chem. Soc. Chem. Commun.* **1989**, 1868.
[13] C. Fouquey, J.-M. Lehn, A.-M. Levelut, *Adv. Mater.* **1990**, *2*, 254.
[14] T. Gulik-Krzywicki, C. Fouquey, J.-M. Lehn, *Proc. Natl. Acad. Sci. USA* **1993**, *90*, 163.
[15] M. Kotera, J.-M. Lehn, J.-P. Vigneron, *J. Chem. Soc. Chem. Commun.* **1994**, 197; M. Kotera, J.-M. Lehn, J.-P. Vigneron, *Tetrahedron* **1995**, *51*, 1953.
[16] M. Suárez, J.-M. Lehn, S. C. Zimmerman, A. Skoulios, B. Heinrich, *J. Am. Chem. Soc.* **1998**, *120*, 9526.
[17] M. J. Brienne, C. Fouquet, A.-M. Levelut, J.-M. Lehn, unpublished results, cited in ref. [2].
[18] J.-M. Lehn, M. Mascal, A. DeCian, J. Fischer, *J. Chem. Soc. Perkin Trans.* **1992**, 461.
[19] J.-M. Lehn, M. Mascal, A. DeCian, J. Fischer, *J. Chem. Soc. Chem. Commun.* **1990**, 479.
[20] E. E. Simanek, X. Li, I. S. Choi, G. M. Whitesides in *Comprehensive Supramolecular Chemistry*, *Vol. 9* (Eds.: J. L. Atwood, J. E. D. Davies, D. D. MacNicol, F. Vögtle, J.-M. Lehn), Pergamon, Oxford, **1996**, Chapter 17.
[21] a) V. Marchi-Artzner, L. Jullien, T. Gulik-Krywicki, J.-M. Lehn, *J. Chem. Soc. Chem. Commun.* **1997**, 117; V. Marchi-Artzner, J.-M. Lehn, T. Kunitake, *Langmuir* **1998**, *14*, 6470; b) V. Marchi-Artzner, F. Artzner, O. Karthaus, M. Shimomura, K. Ariga, T. Kunitake, J.-M. Lehn, *Langmuir* **1998**, *14*, 5164; T. Hasegawo, Y. Hatada, J. Nishijo, J. Umemura, Q. Huo, R. M. Leblanc, *J. Phys. Chem. B* **1999**, *103*, 7505.
[22] M. J. Krische, A. Petitjean, E. Pitsinos, D. Sarazin, C. Picot, J.-M. Lehn, unpublished results.
[23] R. S. Sijbesma, F. H. Beijer, L. Brunsveld, B. J. B. Folmer, J. H. K. Hirschberg, R. F. M. Lange, J. K. L. Lowe, E. W. Meijer, *Science* **1997**, *278*, 1601.
[24] B. J. B. Folmer, E. Cavini, R. P. Sijbesma, E. W. Meijer, *Chem. Commun.* **1998**, 1847; B. J. B. Folmer, R. P. Sijbesma, E. W. Meijer, *J. Am. Chem. Soc.* **2001**, *123*, 2093.
[25] C. P. Lillya, R. J. Baker, S. Hütte, H. H. Winter, Y.-G. Lin, J. Shi, C. Dickinson, J. C. W. Chien, *Macromolecules* **1992**, *25*, 2076.
[26] C.-M. Lee, C. P. Jariwala, A. C. Griffin, *Polymer* **1994**, *35*, 4550; P. Bladon, A. C. Griffin, *Macromolecules* **1993**, *26*, 6604; C. Alexander, C. P. Jariwala, C. M. Lee, A. C. Griffin, *Macromol. Chem. Macromol. Symp.* **1994**, *77*, 283; C. B. St. Pourcain, A. C. Griffin, *Macromolecules* **1995**, *28*, 4116.
[27] C. Hilger, M. Dräger, R. Stadler, *Macromolecules* **1992**, *25*, 2498.
[28] Y. Ducharme, J. D. Wuest, *J. Org. Chem.* **1988**, *53*, 5789.
[29] I. S. Choi, X. Li, E. E. Simanek, R. Akaba, G. M. Whitesides, *Chem. Mater.* **1999**, *11*, 684.
[30] N. Yamaguchi, H. W. Gibson, *Angew. Chem.* **1999**, *111*, 195; *Angew. Chem. Int. Ed.* **1999**, *38*, 143.
[31] W. Yang, X. Chai, L. Chi, X. Liu, Y. Cao, R. Lu, Y. Jiang, X. Tang, H. Fuchs, T. Li, *Chem. Eur. J.* **1999**, *5*, 1144.
[32] a) S. Abed, S. Boileau, L. Bouteiller, N. Lacoudre, *Polymer Bull.* **1997**, *39*, 317; b) S. Abed, PhD Thesis, Université Paris VI (France), **1999**; c) C. He, C.-M. Lee, A. C. Griffin, L. Bouteiller, N. Lacoudre, S. Boileau, C. Fouquet, J.-M. Lehn, *Mol. Cryst. Liq. Cryst.* **1999**, *332*, 251.
[33] T. Kato, M. Fujumasa, J. M. J. Fréchet, *Chem. Mater.* **1995**, *7*, 368; H. Kihara, J. M. J. Fréchet, *Liquid Crystals* **1998**, *24*, 413; H. Kihara, T. Kato, T. Uryu, J. M. J. Fréchet, *Chem. Mater.* **1996**, *8*, 961; T. Kato, H. Kihara, U. Kumar, T. Uryu, J. M. J. Fréchet, *Angew. Chem.* **1994**, *106*, 1728; *Angew. Chem. Int. Ed. Engl.* **1994**, *33*, 1644; T. Kato, O. Ihata, S. Ujiie, M. Tokita, J. Watanabe, *Macromolecules* **1998**, *31*, 3551; T. Kato,

Y. Kubota, M. Nakano, T. Uryu, *Chem. Lett.* **1995**, 1127; T. Kato, M. Nakano, T. Moteki, T. Uryu, S. Ujiie, *Macromolecules* **1995**, *28*, 8875.
[34] R. K. Castellano, D. M. Rudkevich, J. Rebek, Jr., *Proc. Natl. Acad. Sci. USA* **1997**, *94*, 7132.
[35] P. Zhang, J. S. Moore, *J. Polymer Sci.* **1999**, *38*, 207.
[36] W. Jaunky, M. W. Hosseini, J. M. Planeix, A. DeCian, N. Kyritsakas, J. Fischer, *Chem. Commun.* **1999**, 2313.
[37] C. Kaes, M. W. Hosseini, C. E. F. Rickard, B. W. Skelton, A. H. White, *Angew. Chem.* **1998**, *110*, 970; *Angew. Chem. Int. Ed. Engl.* **1998**, *37*, 920.
[38] a) T. L. Hennigar, D. C. MacQuarrie, P. Losier, R. D. Rogers, M. J. Zaworotko, *Angew. Chem.* **1997**, *109*, 1044; *Angew. Chem. Int. Ed. Engl.* **1997**, *36*, 972; b) E. C. Constable, A. M. W. Cargill Thompson, *J. Chem. Soc. Dalton Trans.* **1992**, 3467.
[39] C. D. Eisenbach, A. Göldel, M. Terskan-Reinold, U. S. Schubert, *Macromol. Chem. Phys.* **1995**, *196*, 1077.
[40] M. J. Krische, E. N. Pitsinos, J.-M. Lehn, unpublished results.
[41] CHEM-EQUILI is a computer program for the calculation of equilibrium constants and related values from many types of experimental data (IR, NMR, UV/VIS and fluorescence spectrophotometry, potentiometry, calorimetry, conductometry, etc.). It is possible to use any combination of such kinds of methods simultaneously for reliable calculations of equilibrium constants. For a detailed description see: V. P. Solov'ev, E. A. Vnuk, N. N. Strakhova, O. A. Raevsky, *Thermodynamic of complexation of the macrocyclic polyethers with salts of alkali and alkaline-earth metals* VINITI, Moscow, **1991**; V. P. Solov'ev, V. E. Baulin, N. N. Strakhova, V. P. Kazachenko, V. K. Belsky, A. A. Varnek, T. A. Volkova, G. Wipff, *J. Chem. Soc. Perkin Trans. 2* **1998**, 1489.
[42] a) S.-K. Chang, A. D. Hamilton, *J. Am. Chem. Soc.* **1988**, *110*, 1318; b) S.-K. Chang, D. van Engen, E. Fan, A. D. Hamilton, *J. Am. Chem. Soc.* **1991**, *113*, 7640; c) G. S. Slobodkin, E. Fan, A. D. Hamilton, *New. J. Chem.* **1992**, *16*, 643.
[43] The titration experiment of bis-receptor **1** with cyanurate **4** had to be carried out above 40 °C in chloroform, as **1** undergoes a slow exchange process on the NMR timescale below 40 °C, probably with other rotamers/isomers or even with (an)other nonspecific aggregate(s). Characterization of this phenomenon was not pursued further, as it was only observed in chloroform. In deuterated DMSO, methanol, dichloromethane, or tetrachloroethane, bis-receptor **1** appears as a discrete averaged species in the NMR spectrum. In view of the higher temperature, the association constants determined are lower than those obtained for complexes **13**:**4** or **2**:$\mathbf{4}_3$. Similarly, pure trisreceptor **2** displays a broadened spectrum in chloroform due to the formation of nonspecific intermolecular associations, involving the numerous hydrogen-bonded acceptors and donors, and to conformational diversity. This type of behavior has also been identified in the case of a related oligoisophthalamide strand.[44] Titration of **2** with **4** results in an abrupt sharpening of the peaks.
[44] V. Berl, M. J. Krische, I. Huc, J.-M. Lehn, M. Schmutz, *Chem. Eur. J.* **2000**, *6*, 1938.
[45] a) B. Perlmutter-Haymann, *Acc. Chem. Res.* **1986**, *19*, 90; b) G. Scatchard, *Ann. N.Y. Acad. Sci.* **1949**, *51*, 660; c) A. V. Hill, *J. Physiol.* (London) **1910**, *40*, IV.
[46] V. Ullery, F. Candau, V. Berl, J.-M. Lehn, unpublished results.
[47] a) C. Tranchant, G. Rodier, R. Schmitthaeusler, J. M. Warren, *Rev. Neuro.* **1996**, *152*, 153; b) J. N. Buxbaum, C. E. Tagoe, *Annu. Rev. Med.* **2000**, *51*, 543.
[48] R. Oda, I. Huc, M. Schmutz, S. J. Candau, F. McIntosh, *Nature* **1999**, *399*, 566.
[49] A. Cifferi, in ref. [9], p. 1.
[50] P. J. Flory, *J. Am. Chem. Soc.* **1936**, *58*, 1877.
[51] The derivation of the present treatment was achieved with the assistance of Prof. H. Tsitsishvili, Institute of Cybernetics, Tiflis, Republic of Georgia. The detailed mathematical description of the analytical model will be presented elsewhere along with a discussion of its validity in comparison with other molecular size distribution models for covalent polymers; H. Tsitsishvili, V. Berl, J.-M. Lehn, unpublished results.
[52] H. Günther, *NMR-Spektroskopie*, Thieme, Stuttgart, **1973**.
[53] H. Sillescu, *Kernmagnetische Resonanz*, Springer, Berlin, **1966**.
[54] F. Vögtle, M. Zuber, R. G. Lichtenthaler, *Chem. Ber.* **1973**, *106*, 717.
[55] V. Berl, I. Huc, J.-M. Lehn, A. DeCian, J. Fischer, *Eur. J. Org. Chem.* **1999**, 3089.
[56] J. Otsuki, K. C. Russell, J.-M. Lehn, *Bull. Chem. Soc. Jpn.* **1997**, *70*, 671.
[57] J. P. Collman, J. I. Brauman, J. P. Fitzgerald, P. D. Hampton, Y. Naruta, J. W. Sparapany, J. A. Ibers, *J. Am. Chem. Soc.* **1988**, *110*, 3477.

Received: July 30, 2001 [F3458]

  0947-6539/02/0805-1244 $ 17.50+.50/0